HEAT TRANSFER ENCHANCEMENT IN PIPES USING NANOPARTICLES AND FINS WITH DIFFERENT GEOMETRIES

NESLİHAN EĞERCİ

AUGUST 2025

ÇANKAYA UNIVERSITY

GRADUATE SCHOOL

MECHANICAL ENGINEERING DEPARTMENT
MECHANICAL ENGINEERING MASTER'S THESIS

HEAT TRANSFER ENCHANCEMENT IN PIPES USING NANOPARTICLES AND FINS WITH DIFFERENT GEOMETRIES

NESLİHAN EĞERCİ

AUGUST 2025

ABSTRACT

HEAT TRANSFER ENCHANCEMENT IN PIPES USING NANOPARTICLES AND FINS WITH DIFFERENT GEOMETRIES

EĞERCİ, NESLİHAN
MECHANICAL ENGINEERING MASTER'S THESIS

Supervisor: Assoc. Prof. Dr. Ekin ÖZGİRGİN YAPICI
Co-Supervisor: Prof. Dr. Haşmet TÜRKOĞLU
August 2025, 85 pages

Developing electrical applications in sectors such as energy, electricity, and automotive requires creative approaches to enhance heat transfer. By increasing the heat transfer surface, tube fins in heat exchangers are key components that enhance thermal performance. However, there are several limitations that prevent typical fin designs from achieving optimal performance. Nanoparticles provide more effective heat dissipation by improving system properties and thermal conductivity. Offering greater thermal conductivity than conventional cooling systems, the use of nanofluids enhances heat transfer in tube-fin systems. This study aims to design a finned tube with different geometries and investigate heat transfer using different amounts of fixed-sized nanofluids to achieve the most effective design. Various shapes were examined for the fin study (triangular, rectangular, and circular). Studies found that the triangular finned tube was the most suitable. Different nanostructures are added to the triangular finned structures. Consequently, the optimal nanostructure and pressure expansion are achieved. The best nanoflow was found to be Al_2O_3-TiO_2 with a concentration of 10-6%. The best geometry was found to be a triangular fin.

Keywords: Heat transfer, nanofluid, extended surfaces, optimum design, finned tube

ÖZET

NANOPARTİKÜLLER VE FARKLI GEOMETRİLERE SAHİP KANATÇIKLAR KULLANARAK BORULARDA ISI TRANSFERİ İYİLEŞTİRME

EĞERCİ, NESLİHAN
MAKİNE MÜHENDİSLİĞİ YÜKSEK LİSANS TEZİ

Danışman: Doç. Dr. Ekin ÖZGİRGİN YAPICI
Ortak Danışman: Prof. Dr. Haşmet TÜRKOĞLU
Ağustos 2025, 85 sayfa

Enerji, havacılık ve otomotiv gibi sektörlerde mühendislik uygulamaları geliştirmek, ısı transfer verimliliğini artırmak için yaratıcı yöntemler gerektirir. Isı transfer yüzey alanını genişleterek, ısı eşanjörlerindeki boru kanatçıkları termal performansı artıran temel parçalardır. Ancak, tipik kanatçık tasarımlarının en iyi performansı göstermesini engelleyen birkaç kısıtlama vardır. Nanopartiküller, akışkan özelliklerini ve termal iletkenliği artırarak daha etkili ısı iletimi sağlar. Geleneksel soğutma sıvılarından daha fazla termal iletkenlik sunarak, nanofluidlerin kullanımı boru kanatçık sistemlerinde ısı transferini artırır. Bu çalışmanın amacı, farklı geometrilerde kanatçıklı bir boru tasarımı yaparak en etkili tasarımda farklı konsantrasyonlarda sabit boyutta nanoakışkanlar kullanarak ısı transferini incelemektir. Kanatçık çalışması için çeşitli konfigürasyonlar incelendi (üçgen, dikdörtgen ve daire). Üçgen kanatçıklı borunun en uygun olduğu çalışmalar sonucunda bulundu. Üçgen kanatçıklı yapıya farklı konsantrasyonlarda nano akışlar eklendi. Sonuç olarak en iyi nano akış konsantrasyonu ve geometri yapısı bulundu. En iyi nanoakış Al_2O_3-TiO_2 ve konstrasyonu %10-6' dır. En iyi geometri üçgen yapılı fin olarak bulunmuştur.

Anahtar Kelimeler: Isı transferi, nano akışkan, genişletilmiş yüzeyler, optimum tasarım, kanatçıklı boru

ACKNOWLEDGEMENT

Firstly, I would like to express my sincere thanks to my advisor, Assoc. Prof. Dr. Ekin ÖZGİRGİN YAPICI, for her patient guidance, support, and valuable criticism throughout this study.

I would like to extend my deepest gratitude to my mother and father for their endless love and support under all circumstances; without them, I would not be the person I am today. I am also grateful to my siblings for their constant support and encouragement.

I would also like to thank my friend Yılmaz Ömür ÇAKMAK for his great help and support during the preparation of my thesis.

Finally, I would like to thank everyone who contributed directly or indirectly to this success.

TABLE OF CONTENTS

LIST OF TABLES

LIST OF FIGURES

LIST OF SYMBOLS AND ABBREVIATIONS

SYMBOLS

Δp	: Pressure difference (Pa)
c_p	: Specific heat, (J.kg^{-1}K)
D_h	: Hydraulic diameter, (m)
f	: Friction factor
h	: Heat transfer coefficient, (W.m^{-2}K)
k	: Thermal conductivity, (W.m^{-1}K)
L	: Tube length, (m)
Nu	: Average Nusselt number
$\dot{m}$	: Mass flow rate, (kg/s)
P	: Pressure, (Pa)
Pr	: Prandtl number
PEC	: Performance evaluation criteria
$\dot{q}$	: Heat flux, (W/m^2)
Re	: Reynolds number
T	: Temperature, (K)
U	: Mean velocity, (m/s)
u_*	: Friction velocity
y^+	: Near wall mesh resolution
φ	: Volume concentration of nanoparticle
ρ	: Density, (kg/m^3)
μ	: Viscosity (Pa.s)
τ	: Wall shear stress, (Pa)

ABBREVIATIONS

bf	: Base fluid
d	: Dimple
h	: Hydrodynamic

in	: Inlet
nf	: Nanofluid
m	: Mean
out	: Outlet
p	: Plain
s	: Surface
t	: Thermal
w	: Wall
x	: Location on x-direction
np	: Nanoparticles
k_{eff}	: Effective thermal conductivity of the nanofluid mixture
k_{nf}	: Thermal conductivity of spherical nanoparticles
k_{bf}	: Thermal conductivity of the base fluid
μ_{nf}	: Viscosity of nanofluid
μ_{bf}	: Viscosity of base fluid
V	: Velocity
D	: Diameter
$C_{p,nf}$	: Effective specific heat of the nanofluid
T_w	: Wall temperature
L	: Lenght
W	: Width
α	: Angle

CHAPTER I
INTRODUCTION

1.1 OBJECTIVE OF THE THESIS

Innovative approaches to heat transfer processes are now required due to rising energy demands and high efficiency requirements in thermal engineering applications. In the light of the above, the study aims to examine the potential for enhancing heat transfer in circular pipes by utilizing nanofluids and fins of different geometries. Nanoparticles in a liquid create nanofluids, which are used in modern engineering applications because of their exceptional heat transfer capabilities and high thermal conductivity [1-3]. The aim of this research is to increase system performance, reduce energy consumption and increase heat transfer efficiency by using nanofluids at different concentrations in laminar flow and using the finned tube with the best geometric structure [4,5].In addition, the integrated effects of nanofluids on extended surfaces in tubes is also investigated since finned tubes provide significant improvements in heat transfer by increasing the surface area, regulating the flow and promoting turbulence depending on the geometric configurations of the fins [6,7]. Within the scope of the research, the effects of nanofluids on heat transfer examined in detail and the flow and heat transfer in horizontal circular pipes with different geometric structures analyzed in these investigations conducted using Computational Fluid Dynamics (CFD) simulations, the factors affecting the performance of nanofluids such as nanoparticle type, concentration and size evaluated in detail [8,9]. By demonstrating the potential of nano fluids in engineering applications, this study seeks to aid in the creation of novel solutions that offer energy efficiency. One significant result of this research will be the development of more sustainable and efficient energy solutions, particularly in industrial systems like channel pipes, using nanofluids and geometrical modifications [10].

1.2 LITERATURE SURVEY

1.2.1 Literature Review on Nanofluids

For improving the heat transfer of conventional fluids, nanoparticles can be used to prepare nanofluids. The fluid's surface area and thermal capacity are raised by the inclusion of nanoparticles, which significantly enhances heat transfer efficiency [11]. The main physical phenomena that are highlighted are as follows [12]:

- Increase in the effective thermal capacity of the fluid,
- Inter-particle interactions expand the fluid surface,
- Increase in the intensity of turbulence and turbulence in the fluid,
- Flattening of the temperature gradient of the fluid by scattering of nanoparticles.

Since conventional techniques of heat removal are frequently insufficient, heat dissipation is essential in systems like electrical components and car radiators. When compared to traditional fluids, the efficiency of heat transfer has been greatly increased by the development of nanofluids, which are colloidal mixes of nanoparticles in base fluid [13]. Initially identified by Granqvist et al. [14], these nanoparticles enhance thermal conductivity due to factors like Brownian motion and reduced thermal boundary layers. Choi [6] was the pioneer in introducing nanofluids, demonstrating their superiority in heat transfer. Researchers have explored various modifications in radiator geometries and coolant compositions to enhance performance, finding that nanofluids can lead to smaller, lighter radiators with better heat transfer capabilities, ultimately reducing fuel consumption and increasing vehicle efficiency [15].

The impacts of nanofluids in different heat exchangers—which are crucial for preserving the ideal working temperatures in industrial machinery, water, chemicals, and oils—have been thoroughly investigated by researchers. It has been demonstrated that using nanofluids improves these heat exchangers' efficiency [16]. The demand for efficient heat elimination in modern electronic devices, which require high power density and miniaturization, has led to findings that liquid-cooled systems are more compact and effective than air cooling due to their superior thermal properties.

Research has indicated that staggered geometries in heat sinks offer improved performance, with triangular pin fins outperforming other shapes. The combination of nanofluids and innovative heat sink designs has garnered significant attention in the cooling of electronics [17].

Engineering materials made by distributing nanometer-sized particles in a base fluid are included in nanofluid technology to be used for heat transfer enhancement in energy systems, biomedical applications, industrial processes etc. The fields of fluid mechanics, thermodynamics, and nanotechnology are all combined in the scientific foundation of nanofluids. Compared to traditional fluids, these materials provide better control over viscosity and thermal conductivity. Large surface areas and Brownian motion raise the convective heat transfer coefficient, resulting in more efficient heat management [18].

Compared to solids, liquids like water, ethylene glycol, and motor oil have lower heat conductivity. Adding tiny solid particles to fluids can boost their heat conductivity. However, there have been drawbacks to this approach in certain heating and cooling systems [19]. Millimeter and macro-meter sized particles may form a sediment layer on the lower surface of the fluid after mixing, which may reduce the heat transfer capacity. When the flow rate of the fluid is increased, sedimentation decreases, while there is a greater risk of erosion. Large particles may block the flow channels when the cooling channels are narrow. In addition, the pressure drops in the fluid increases after mixing, increasing the pump power required for the system to operate.

Traditionally, particle mixing of fluids has not been preferred; however, thanks to modern material production methods, it has become possible to produce nanoparticles with different properties. This development has made mixing of fluids with solid particles common in heat transfer. Heat transfer fluids are generally liquids such as water, engine oil and ethylene glycol, and their low heat transfer performance negatively affects the efficiency of the system. The use of nanoparticles smaller than 100 nanometers is seen as an important step to increase the performance of heat transfer fluids [20]. The contributions of nanofluids to thermal systems are as follows [21]:

- The use of nanofluids is driven by the need to increase heat transfer rate and system performance. The thermal conductivity and surface area of these fluids are higher than typical fluids.
- Increased heat transfer and thermal conductivity allow systems to be designed in smaller sizes, thus reducing costs and increasing efficiency.
- The lightness of nanosized particles minimizes sedimentation.

- The size of these particles reduces the force applied to the surfaces and wear, extending system life.

  In addition, nanosized particles prevent blockage in microchannels

Technological developments and increasing energy demand have led scientists to seek alternative energy sources and to use existing energy more efficiently so various methods are being studied to improve heat transfer. Maxwell's studies in the late 1800s focused on adding metal and non-metal particles, which have higher thermal conductivity than liquid fluids, to liquid fluids. However, this method caused negative effects such as sedimentation and channel blockage due to the large size of the particles and negatively affected system performance [13]. Nanoparticles produced through nanotechnology provided the opportunity to continue Maxwell's work. Choi, using the term nanofluid, showed that nanoparticles added to small volumes of liquid increased thermal conductivity two-fold [6]. These findings revealed the need for diversity in production methods suitable for the needs of heat transfer systems. There are two basic methods in the production of nanofluids, and these are: single step and two step methods. While the single step method is based on the direct production of nanoparticles in the base liquid fluid, this method was developed by Akoh et al. [22]. The two-step method is based on the combination of nanoparticles previously obtained by different techniques (e.g. chemical vapor condensation or hydrogen reduction) with the base fluid using appropriate suspension methods [23]. There are two important methods for producing nanofluids. The first of these, the “Two-Step Method”, is where nanoparticles are produced in powder form by physical or chemical methods and then mixed with liquid by methods such as magnetic force, ultrasonic agitation, high shear mixing, homogenization and ball milling, enabling large-scale and economical production [24].

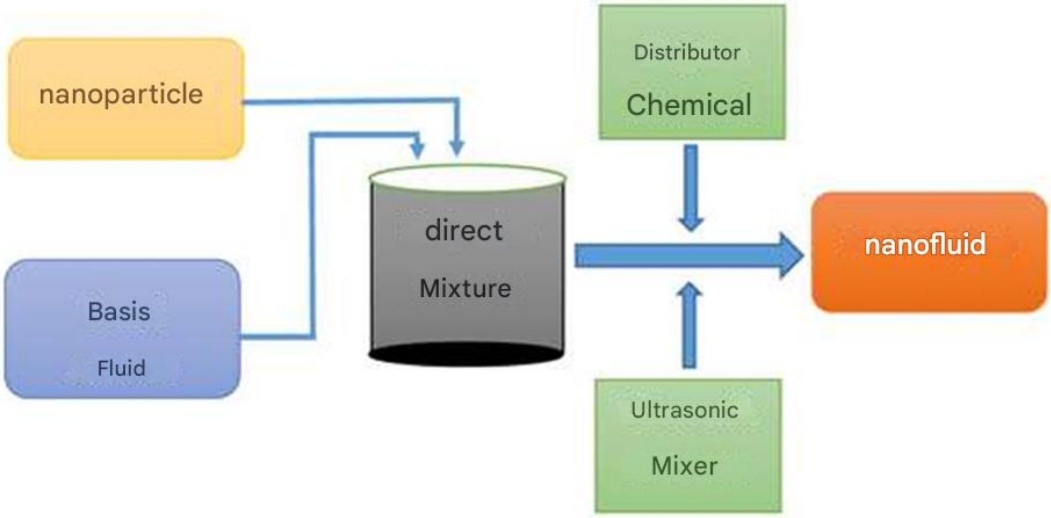

Figure 1: Schematic representation of the two-step method [25]

Since it is difficult to obtain a stable liquid in the two-step method, different preparation methods were needed and, in this context, the single-step method was developed [26]. “Single Step Method” The single-step method was developed to make the unstable structure of the two-step method more stable and to reduce sedimentation. The fluid's enhanced stability and the avoidance of particle aggregation are the method's advantages. Direct vapor condensation, chemical vapor condensation, and single-step chemical synthesis are a few techniques employed in the single-step approach [27]. Due to its high cost, the two-step method is currently used even though the single-step method provides the chance to create more homogenous nanofluids [28].

To improve the stability of nanofluids, it's important to keep the pH away from the isoelectric point (IEP), where stability decreases. A strong repulsive force maintains stability, and the correct pH helps nanoparticles disperse well. Research shows that at a neutral pH of around 7, carbon nanotubes (CNTs) clump, but extreme pH levels can cause corrosion in heat transfer uses. During heating and cooling, particles may stick together, so stability is crucial at high temperatures. Many nanofluids use surfactants and polymers for stabilization, but these can break down under high heat, impacting stability [29,30]. It is crucial for nanofluids to remain stable across a wide temperature range for effective heat transfer applications. Studies indicate significant agglomeration and deterioration at elevated temperatures, with Chang et al. [31] noting an increase in nanoparticle clustering and a decrease in zeta potential, indicating reduced stability. High-pressure homogenization and plasma treatment are effective methods for improving high-temperature stability and surface functionalization. Tavares et al. created a stable Cu-EG nanofluid using plasma treatment without surfactants, maintaining stability up to 150 °C, but agglomeration occurs at 197 °C due to increased particle activity; these agglomerates can be broken up using ultrasonication. Sani et al. [32] developed a stable ethylene glycol-based nanofluid with single wall carbon nanohorns using high-pressure homogenization, maintaining stability for six months at temperatures up to 150 °C. Stability is important for heat transfer of nanofluid, and when CTAB, SDS, tannic acid ammonia solution, SDBS and sodium deoxycholate substances were tested, it was determined that the type of surfactant and the mixing time affected the stability [33].

One of the primary determinants of the thermal performance of nanofluids is the impact of nanoparticle concentration on heat transfer. Because of their high surface area and density difference, which form a strong thermal bridge in the fluid, nanoparticles enhance heat transmission by raising the base fluid's thermal conductivity. Additionally, the micro-convection effect and Brownian motion provide for the quick spread of heat energy. On the other hand, when a specific concentration is exceeded, undesirable consequences like increased viscosity and sedimentation could happen, which could lower system efficiency and have a detrimental impact on heat transfer [34].

In fact, the effects should be examined based on the results of the research. Pak and Cho [35] used Al2O3 nanoparticles with a size of 13-27 nm and pure water as the base fluid in their experimental study. They stated that the heat transfer coefficient increased by 45% at a particle concentration of 1.34% and by 75% at a particle concentration of 2.75%.

Arıcı et al. [36] reported in their numerical study that they added Cu nanoparticles to the water base fluid in a trapezoidal cavity with a moving upper wall in which an adiabatic square block was placed; that heat transfer increased with the addition of nanoparticles to the fluid and the decrease of the Richardson number, and that more heat transfer occurred with the enlargement of the adiabatic square block, independent of the nanoparticle concentration and Richardson number.

Akçaoğlu et al. [37] numerically investigated the natural convection of Cu, Al_2O_3 nanoparticles and water-based nanofluids in a compartmented square closed environment; they reported that heat transfer increased with increasing nanoparticle concentration and Rayleigh number. Öğüt [38] numerically investigated the natural convection of Cu, Ag, Al_2O_3 nanoparticles and water-based nanofluids in an inclined square; they reported that the inclination angle affected the heat transfer rate, and heat transfer increased with increasing nanoparticle concentration and Rayleigh number.

Xuan and Lee [39] showed in their experimental study with 100 nm Cu nanoparticles that the heat transfer coefficient increased as well as decreased with the addition of nanoparticles, and that viscosity, particle size, particle properties and base fluid were also important in the thermal conductivity of the nanofluid.

Öğüt [40] investigated the natural convection of water-based nanofluids in a partially heated, inclined square closed environment with constant heat flux from the side wall and observed that the heat transfer rate decreased as the heater length increased.

Abu-Nada et al. [41] reported that heat transfer increased with the addition of nanoparticles by adding Cu, Ag, Al_2O_3 and TiO_2 nanoparticles to the water base fluid in a cylindrical cavity, and that the nanofluid prepared with Al_2O_3, which has very low thermal conductivity, gave the highest average Nusselt values, and that this was attributed to the very low thermal diffusivity value of Al_2O_3 nanoparticles.

Susantez and Kahveci [42] reported that heat transfer increased with the addition of nanoparticles and the increase in the Rayleigh number of the sides of the water base fluid in a square cavity with a conductive circular block inside, and that heat transfer decreased with the increase in the diameter of the conductive block. In the numerical study conducted by Ghasemi and Aminossadati [43], the heat transfer of nanofluid prepared with water and Al2O3 nanoparticles in a triangular cavity with a moving wall was investigated. They showed that the heat transfer increased with the addition of nanoparticles and the movement of the wall.

1.2.2 Literature Review on the Impact of Fins on Heat Transfer

Heat exchangers' primary goal is to maximize heat transfer between fluids to save energy and operate efficiently. Applying extended surfaces, which are named as fins, is one of the most used passive geometrical heat transfer enhancement methods, especially for internal flow. Although fins are efficient in transferring heat from the pipe surface to the surrounding fluid, their contribution to heat transfer is still limited and heat loss at the end points may reduce as fin length increases [44]. Fin efficiency and fin efficiency coefficient are used to assess how fins affect heat transmission. Fin efficiency compares a fin's actual performance to the greatest heat transfer that is theoretically possible.

To enhance the heat transfer surface using fins, numerous investigations have been carried out. For example, El Maakoul et al. [45] investigated the thermohydraulic performance of a double pipe heat exchanger with longitudinal fins, focusing on the impact of fin type on thermal performance. The study demonstrated that split longitudinal fins resulted in a higher heat transfer rate compared to traditional longitudinal fins. Additionally, Hosseini et al. [46] examined the effects of longitudinal fins in double-pipe heat exchangers containing phase change materials through both experimental and numerical methods, comparing two different fin heights to assess their influence on the thermal performance of the heat exchanger. The results showed that the fin length shortens the melting time of the phase change material.

Kim et al. [47] conducted experimental and numerical studies on thermal resistance values in finned tubular heat exchangers, exploring various pipe size ratios, spacing between fins, and fin types, confirming that numerical results aligned with experimental findings.

Kotcioğlu and Bölükbaşı [48] tested flat surface fins, cylindrical fins, and channel elements at 60-degree angles, finding cylindrical and flat fins performed well in heat transfer, with increased Reynolds numbers enhancing this transfer.

Erek et al. [49] numerically examined the impact of spacing between fins, displacements at the pipe center, fin height, pipe thickness, and ellipticity on heat transfer and pressure drop across ten heat exchangers.

Şahin et al. [50] investigated the heat transfer effects of fins in flat-tube heat exchangers using the finite volume method, finding a 105.24% increase in total heat transfer with 300-degree angled fins. Bazarbashi [51] focused on multi-objective optimization of a corrugated fin heat exchanger, calculating heat transfer and pressure drop characteristics using Response Surface Methodology (RSM) for different fin arrangements, which yielded results consistent with existing literature for Nusselt number and friction factor predictions.

Buyruk and Karabulut [52] numerically evaluated the thermal performance of rectangular fins at 30° and 90° angles with a 10 mm horizontal offset in a plate heat exchanger, finding a 10% increase in heat transfer at the 30° fin angle compared to a channel without fins. Buyruk and Karabulut [53] also examined the impact of different Reynolds numbers and fin heights on heat transfer in both parallel and counterflow conditions, noting an 8.4% temperature increase at the outlet in counterflow with zigzag fin channels compared to straight channels, and a 7.6% increase in parallel flow.

Karataş [54] conducted a study on heat exchange in body-tube type heat exchangers using Computational Fluid Dynamics (CFD) to analyze flow and heat transfer coefficients alongside pressure losses with various flow types and zigzag plate models.

Cüce [55] examined the effects of conventional and slotted longitudinal fins on heat transfer and found that slotted fins were more effective in heat transfer per unit volume. In addition, it was observed that the slots reduced the weight of the fins and their effects became more pronounced at low convection coefficients.

Koca and Budak [56] experimentally investigated the effects of the finned inner tube on heat transfer in a concentric tube heat exchanger and found that the highest heat transfer occurred in the tube with a higher number of fins. It was determined that the heat transfer in the 300 mm long finned section was 147.38% higher than in the straight tube, and the pressure drop was 131.25% lower.

Işık and Tuğan [57] studied heat transfer with straight and wavy copper fins on pipe surfaces across four different flow rates, concluding that wavy fins enhanced heat transfer by 8% to 11% compared to straight fins. Additionally, Buyruk ve Karabulut [58] examined the effects of zigzag and internal-external zigzag fins on heat transfer at 300, 600, and 900 Reynolds numbers, noting a 9% increase in heat transfer for B-type finned channels compared to a channel without fins.

Tepe [59] analyzed the effect of cavity/pertusion fins on heat transfer and flow characteristics in finned tubular heat exchangers using Ansys Fluent, revealing that such fins could improve heat transfer by up to 26.63% compared to flat fins. Parlak and Çelik [60] investigated rectangular fins arranged in a single microchannel with water as the fluid, demonstrating that pressure drop and Nusselt number increased with higher Reynolds numbers and additional fins.

Abdulateef et al. [61] experimentally and numerically analyzed the effects of longitudinal fins in a three-tube heat exchanger, discovering that triangular fins improved phase change material melting times by 11%, 12%, and 15% compared to longitudinal fins.

Kazemi et al. [62] researched the impact of fin angles on heat transfer during phase change, noting that increasing the angle in three-finned heat exchangers reduced melting time while altering angles in two-finned exchangers had mixed effects.

1.2.2.1 Heat Transfer for Laminar Flow in Finned Pipes

Fins improve heat transfer by increasing the pipe surface area, but the heat transfer coefficient is low in laminar flow due to low turbulence. Therefore, the effectiveness of fins is more limited than in turbulent flow. The temperature gradient and heat transfer path on the finned surfaces are directly related to fin effectiveness. Fins made of materials with high thermal conductivity allow heat to be transferred more efficiently from the pipe surface to the surrounding fluid [63].

In laminar flow regions, the optimum design of fins is determined by geometric parameters such as fin height, spacing and thickness. High-density fin arrangements may limit the heat transfer coefficient by increasing the flow resistance due to boundary layer interactions. However, fins that provide a large surface area even at low Reynolds numbers provide an advantage by increasing heat transfer in heat exchangers operating against air [64]. Internally finned pipes are extensively used in heat exchangers to enhance heat transfer by providing additional surface area. Initial studies, both analytical and experimental, focused on laminar flow and heat transfer in pipes with uniform fin heights. These studies yielded findings on velocity distribution, friction factor, temperature distribution, Nusselt number, and the effect of fin conductance on heat transfer performance. The heat transfer effectiveness of internally finned pipes is influenced by factors such as fin conductance, heat transfer surface extension, and the local heat transfer coefficient, which are interdependent. To enhance fin conductance, increasing thickness while reducing height is essential. However, to maintain lightweight designs in heat exchangers, fin thickness should be minimized. Increasing fin surface area can improve heat transfer but also raises the friction factor, leading to higher energy requirements for fluid pumping through the pipe. The local heat transfer coefficient is influenced by the shape and spacing of fins. Numerous studies have explored optimizing finned surfaces to enhance heat transfer efficiency while minimizing the size and weight of internally finned pipes. These efforts have led to the identification of profiles that maximize heat transfer per unit length or surface area. However, these optimal profiles are complex to manufacture, and there is insufficient information available regarding the coefficient of friction, which is expected to be relatively high [65].

In the light of above the study aims to examine the potential for enhancing heat transfer in circular pipes by utilizing different nanofluids at different concentrations and fins of different geometries and dimensions.

CHAPTER II

MATHEMATICAL MODELING

2.1 INTRODUCTION

In this section, mathematical formulations for enhancing heat transfer efficiency in internal pipe flows using nanofluids are discussed. The use of nanofluids offers a promising approach to improving heat transfer efficiency in various fluid flow scenarios.

2.2 MATHEMATICAL EQUATIONS

The mathematical equations in this section are crucial for understanding the fundamental principles behind the enhancement of heat transfer in nanofluid filled systems. The governing equations have been derived, considering the effects of nanoparticle concentration, fluid flow characteristics, and geometric design on heat transfer performance. These mathematical models can be used to describe the complex interactions between nanofluids and system components, helping to understand the mechanisms underlying the improvement in heat transfer.

2.3 NANOFLUID MODELING

Nanofluids can be modeled and formulated using two widely accepted methods. To explain, nanofluids consist of nanoscale metallic particles such as Al_2O_3, TiO_2, Cu, and MXene dispersed in a base fluid like water, ethylene glycol, or oil. In this study, water was selected as the base fluid and mixed with nanoparticles of Al_2O_3, TiO_2, Cu, and MXene for analysis.

There are two main approaches for modeling nanofluid flow: single-phase and multi-phase models. The single-phase model is based on the assumption that nanoparticles move at the same velocity as the base fluid and maintain thermal equilibrium. This approach assumes that the nanoparticles are homogeneously distributed within the base fluid, and the thermophysical properties of the nanofluid are calculated using equations found in the literature. Since its inception, multi-phase (i.e., liquid–liquid, gas–liquid, and liquid–liquid–gas) flow reactors have served as the foundation of microfluidics, particularly as an effective method of preventing channel clogging when working with solids.

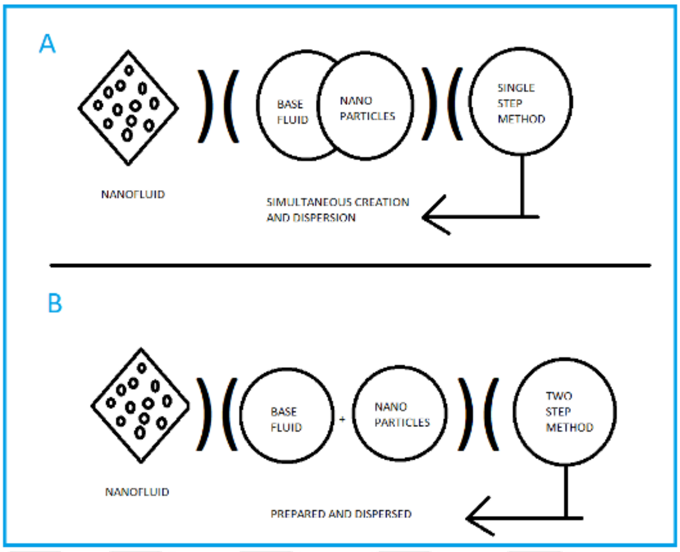

Figure 2: Different methods of preparation nano fluids [66,67]

2.3.1 Single-Phase Model for Nanofluids

The single-phase model is a widely recognized and commonly used approach for nanofluid flow studies; therefore, analyses in this study were conducted using the single-phase model. The advantage of the single-phase model is that, since the nanoparticles dispersed in the base fluid are at the nanoscale, it is easy to assume that these nanoparticles are homogeneous with the base fluid. In other words, it can be assumed that they are in thermal equilibrium and share the same velocity.

2.3.2 Multi-Phase Modeling

In practical applications, nanoparticles are often not homogeneous, and the velocities of nanoparticles and the base fluid in the flow field may differ. Achieving thermal equilibrium can also be challenging. Well-known multi-phase models for calculating nanofluid flows include the Eulerian-Mixture model and the Eulerian-Eulerian model [68]. In the first model, the Eulerian-Mixture model, the governing equations of fluid dynamics are solved by correlating the velocity terms of nanoparticles and the base fluid and then averaging them. In the Eulerian-Eulerian model, the governing equations for nanoparticles and the base fluid are solved separately, with their velocity terms correlated and solved individually**.**

2.4 THERMOPHYSICAL PROPERTIES OF NANOFLUIDS

In the analyses conducted in this study, the results were examined using three different nanofluid mixtures. These nanofluids were mixed with water at specific concentrations. The results examined are detailed in the following chapters. A single-phase flow model was used in the study, focusing on calculating the most effective thermal properties of the concentration and based on the assumption of homogeneity between the nanoparticles and the base fluid.

2.4.1 Density of Nanofluids

The density of the nanofluid was determined using the following formula which can be applied for various volume concentrations [35].

$$\rho_{nf}=(1-\varphi)\rho_{bf}+\varphi\rho_{np} \tag{2.1}$$

Below correlation shows applicability in the density and volume concentration range of the nanofluid mixture [69].

$$\rho_{nf}(C_p)_{nf}=\varphi_{np1}\rho_{np1}C_{p_{np1}}+\varphi_{np2}\rho_{np2}C_{p_{np2}}+\left(1-\varphi_{np1}-\varphi_{np2}\right)\rho_{bf}(C_p)_{bf} \tag{2.2}$$

where ρ_{nf} φ, *bf*, C_p and *np* resort to density of nanofluid, volume concentration, base fluid, specific heat of the nanofluid and nanoparticles, respectively.

2.4.2 Specific Heat of Nanofluids

The effective specific heat of the nanofluid, $(C_p)_{nf}$ is calculated using the equation below [70].

$$(C_p)_{nf}=\frac{(1-\varphi)(\rho C_p)_{bf}+\varphi(\rho C_p)_{np}}{\rho_{nf}} \tag{2.3}$$

where φ, *bf*, and *np* resort to volume concentration, base fluid and nanoparticles, respectively.

2.4.3 Thermal Conductivity of Nanofluids

Thermal conductivity of nanofluids depend on quite a lot of parameters as seen in Figure 3.

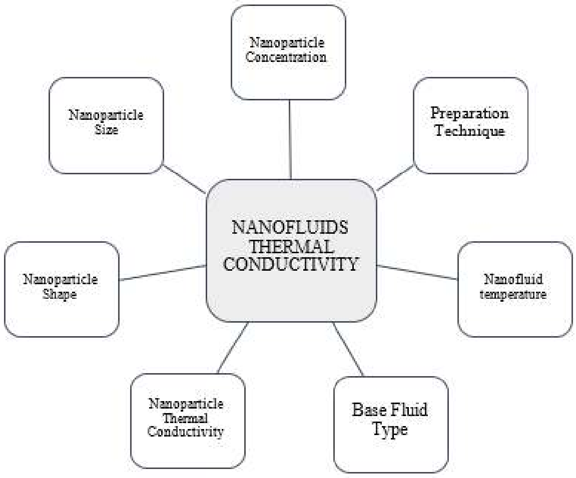

Figure 3: The most effective thermal conductivity parameters on nano-fluids [71].

The Maxwell's model for evaluating the thermal conductivity is shown below:

$$k_{nf} = \frac{k_{np}+2k_{bf}-2\varphi(k_{bf}-k_{np})}{k_{np}+2k_{bf}+\varphi(k_{bf}-k_{np})}k_{bf} \tag{2.4}$$

The analysis of measurements for a mixture consisting of three components shows that the two-phase fluid is treated as a single liquid mixture k_{bf}, the situation can be approached using different methodologies. A simple and practical method involves modifying an equation originally designed for two components to account for the presence of three components. The equation used in this study is a generalized version of Maxwell's equation, derived through a methodology similar to that employed [72].

k_{nf}, k_{np}, k_{bf}, φ which respectively represent the thermal conductivity of the nanofluid, thermal conductivity of nanoparticles, thermal conductivity of the base fluid, volume fraction (concentration) of nanoparticles.

$$k_{eff} = k_{bf}[1 + \frac{3\varphi_1\frac{k_{nf1}-k_{bf}}{2k_{bf}+k_{nf1}}+3\varphi_2\frac{k_{nf2}-k_{bf}}{2k_{bf}+k_{nf2}}}{(1-\varphi_{np1}-\varphi_{np2})+3\varphi_1\frac{k_{bf}}{2k_{bf}+k_{nf1}}+3\varphi_2\frac{k_{bf}}{2k_{bf}+k_{nf_2}}}] \tag{2.5}$$

k_{eff}, k_{nf}, k_{bf} and φ which respectively represent the effective thermal conductivity of the nanofluid mixture, thermal conductivity of spherical nanoparticles, the thermal conductivity of the base fluid, and the volume concentration.

2.4.4 Viscosity of Nanofluids

The viscosity of nanoparticles is a key parameter in determining the flow behavior and energy transfer efficiency of nanofluid systems. The mathematical formulas are provided in the table below.

Table 1: The mathematical formulas for the viscosity of nanofluids

The effective viscosity	$\mu_{nf} = \mu_{bf}(1 + 2.5\varphi)$
The viscosity of Al_2O_3 is predicted by the model	$\mu_{nf} = \mu_{bf}(1 + 39.11\varphi_{np} + 533.9\varphi^2_{np})$
Viscosity of TiO_2	$\mu_{nf} = \mu_{bf}(1 + 5.45\varphi_{np} + 108.2\varphi^2_{np})$
An effective viscosity prediction model	$\mu_{nf} = \mu_{bf}(1 + 2.5\varphi_{np} + 6.2\varphi^2_{np})$

Where, μ_{nf} viscosity of nanofluid, μ_{bf} viscosity of base fluid, respectively.

2.5 IMPORTANT PARAMETERS OF FLUID FLOW

2.5.1 Reynolds Number

The Reynolds number is the ratio of inertial forces to viscous forces in any flow and is one of the most important parameters for characterizing fluid flow. The Reynolds number is defined as:

$$Re = \frac{\rho_{nf} U D_h}{\mu_{nf}} \tag{2.6}$$

Where ρnf is the density of the nanofluid (kg/m^3). V is the velocity of the nanofluid (m/s), D is the diameter of the flow channel (m). μnf (pa.s) is the dynamic viscosity.

2.5.2 Nusselt Number

The Nusselt number is considered a standard way to express the rate of heat transfer between a fluid and a solid surface, and it has a physical significance for both convective and conductive heat transfer within a liquid layer [73].

$$Nu = \frac{h D_h}{k_{nf}} \tag{2.7}$$

Here, h, k_{nf}, and D_h are the heat transfer coefficient, thermal conductivity, and hydraulic diameter of the pipe, respectively. The local Nusselt number can be calculated using the following formula:

$$Nu_x = \frac{h_x D_h}{k} \tag{2.8}$$

$$h_x = \frac{\dot{q}_s}{T_w - T_m(x)} \quad (2.9)$$

where $q\square_s$ is the heat flux applied on the outer surface, $T_m(x)$ the mean temperature of the fluid and T_w the wall temperature.

$$T_m(x) = T_{m,in} + \frac{\dot{q}_s \pi D_h}{\dot{m} C_p} x \quad (2.10)$$

Here, D_h, $T_{m,i}$, $m\square$, C_p, and x represent the hydraulic diameter of the pipe, average inlet temperature of the fluid, mass flow rate, specific heat capacity, and the distance from the inlet of the dimpled pipe, respectively. The average number of Nusselt can be calculated as follows:
The Overall Nu is calculated as:

$$\bar{Nu} = \frac{1}{L}\int_0^L Nu(x)dx \quad (2.11)$$

2.5.3 Friction Factor

It is calculated using the Darcy friction factor for Laminar flow in pipes [73].

$$f = \frac{2D_h \Delta p}{\rho_{nf} L U^2} \quad (2.12)$$

f, D_h, Δp, ρ_{nf}, L, U represent the Darcy friction factor, hydraulic diameter of the pipe/channel, pressure drop along the pipe, density of the nanofluid, length of the pipe, average velocity of the fluid, respectively.

The friction factor can also be obtained by substituting the wall shear stress τ. The Darcy friction factor is:

$$f = \frac{8\tau_w}{\rho_{nf} U^2} \quad (2.13)$$

For laminar flow;

$$f = \frac{64}{Re} \quad (2.14)$$

2.5.4 Entrance Length

To guarantee the total advancement of the stream field hydrodynamically and thermally, it is imperative to calculate the fundamental entrance length for laminar and turbulent pipe flow systems. Within the case of laminar stream, the hydrodynamic and thermal entrance lengths can be calculated as follows [73];

$$L_{h,laminar} \approx 0.05ReD \tag{2.15}$$

$$L_{t,laminar} \approx 0.05RePrD \tag{2.16}$$

2.5.5 Performance Evaluation Criteria

To evaluate the overall effects of heat transfer and pressure drop on the thermal performance of the pipe flow, performance evaluation criterion (PEC) is defined such as [74];

$$PEC = \frac{\frac{Nu_f}{Nu_p}}{\left(\frac{f_f}{f_p}\right)^{\frac{1}{3}}} \tag{2.17}$$

Where Nu_f, Nu_p , f_f and f_p are respectively Nusselt Number of fins, Nusselt number of plain tubes, Friction factor of fins and friction factor of plain tube.

CHAPTER III
NUMERICAL METODOLOGY

3.1 GOVERNING EQUATIONS

The governing equations for the current physical problem are derived from fundamental principles of thermodynamics and heat transfer, encompassing Newton's Second Law, the Law of Conservation of Energy, and the principle of mass conservation. The following simplifying assumptions are made for the analysis:

- The flow and heat transfer are considered steady, laminar, three-dimensional, and incompressible.
- The fluid behaves as a single-phase substance.
- The thermophysical properties of both the fluids and solid phases remain constant.
- The impact of thermal radiation and magnetic forces are negligible.

The inlet and outlet points are pre-defined. Calculations of the governing equations are performed using thermal properties, as outlined in the assumptions above.

3.1.1 Continuity Equations

The continuity equation, based on the principle of mass conservation, is a fundamental principle of fluid mechanics. It states that matter within a fluid system remains constant, regardless of the flow characteristics. Compared to others, the continuity equation more clearly states that the net mass flow into a control volume is equal to the net mass flow out of that volume [75]

$$\frac{\partial u}{\partial x} + \frac{\partial v}{\partial y} + \frac{\partial w}{\partial z} = 0 \tag{3.1}$$

$$\nabla.(\rho V) = 0 \tag{3.2}$$

3.1.1.1 General Continuity for Incompressible Flow

The Continuity for Incompressible Flow equation shows that the fluid is not "volumetrically compressed" at a certain location, in which case the inlet and outlet flow rates are balanced. It is used in numerical methods and is one of the basic conditions for ensuring the physical consistency of the flow field. For example, in CFD analyses, this equation is used. [75]

3.1.2 Momentum Equations

Momentum equations, also known as Navier-Stokes equations, are simply an expression of Newton's second law of motion, representing the incompressible on the fluid within a slice of the pipeline cross-section. [75] In this study, the equations were not solved analytically. They were solved using Ansys Fluent.

3.1.2.1 Navier-Stokes Equations

Viscous motions in a fluid that comply with Newton's law are defined by the Navier-Stokes equations. These equations represent the differential form of momentum conservation, specifically within a control volume. In Cartesian coordinates, the equations are expressed as follows:

r component:

$$\frac{\partial v_r}{\partial t} + v_r \frac{\partial v_r}{\partial r} + \frac{\partial w}{\partial z} + \frac{v_\theta}{r}\frac{\partial v_r}{\partial r} - v_\theta^2 \frac{\partial v_r}{\partial z} = fr - \frac{1}{p}\frac{\partial p}{\partial r} + v[\frac{\partial}{\partial r}\left[\frac{1}{r}\frac{\partial}{\partial r}(r v_r)\right] + \frac{1}{r^2} + \frac{\partial^2 v_r}{\partial \theta^2} - \frac{2}{r^2}\frac{\partial v_\theta}{\partial \theta} + \frac{\partial^2 v}{\partial z^2} \tag{3.3}$$

∂ component

$$\frac{\partial v_\theta}{\partial t} + v_r \frac{\partial v_\theta}{\partial r} + \frac{v_\theta}{r}\frac{\partial v_\theta}{\partial \theta} + \frac{v_r v_\theta}{r} + w\frac{\partial v_\theta}{\partial z} = fr - \frac{1}{pr}\frac{\partial p}{\partial \theta} + v[\frac{\partial}{\partial r}\left[\frac{1}{r}\frac{\partial}{\partial r}(r v_\theta)\right] + \frac{1}{r^2} + \frac{\partial^2 v_\theta}{\partial \theta^2} - \frac{2}{r^2}\frac{\partial v_r}{\partial \theta} + \frac{\partial^2 v_\theta}{\partial z^2} \tag{3.4}$$

z component:

$$\frac{\partial w}{\partial t} + v_r \frac{\partial w}{\partial r} + \frac{v_\theta}{r}\frac{\partial w}{\partial \theta} + w\frac{\partial w}{\partial z} = fz - \frac{1}{p}\frac{\partial p}{\partial z} + v\left[\frac{1}{r}\frac{\partial}{\partial r}\left(r\frac{\partial w}{\partial r}\right) + \frac{1}{r^2} + \frac{\partial^2 w}{\partial \theta^2} + \frac{\partial^2 w}{\partial z^2}\right] \tag{3.5}$$

In incompressible flows, assuming constant density, the unknown terms in the equations are the velocity components in the x, y, and z directions, as well as the pressure value. The motion of the flow is described by a total of four equations: the continuity equation and three momentum equations. Navier-Stokes and continuity equations are discretized and solved numerically to determine the four unknown values mentioned above. The flow problem is defined within the numerical solution using boundary and initial conditions, and results are obtained for each point where discretization is applied.

3.1.3 Energy Equations

The energy equation is based on the principle of conservation of energy, also known as the first law of thermodynamics. This principle states that energy cannot be created or destroyed within a system but only transformed from one form to another. The energy equation, based on this principle, examines the energy changes within a system and considers factors such as heat transfer, work, and internal energy interactions [75].

$$\rho \frac{DT}{Dt} = \nabla\ (k\nabla T) + \dot{q} + \varphi \tag{3.6}$$

$$\frac{DT}{Dt} = \frac{\partial}{\partial t} + v_r \frac{\partial}{\partial r} + \frac{v_\theta}{r}\frac{\partial}{\partial \theta} + \mathrm{w}\frac{\partial}{\partial z} \tag{3.7}$$

$$\nabla.(\ k\nabla T) = \frac{1}{r}\frac{\partial}{\partial r}\ (rk\frac{\partial T}{\partial r}) + \frac{1}{r^2}\frac{\partial}{\partial \theta}(k\frac{\partial T}{\partial \theta}) + \frac{\partial}{\partial z}(k\frac{\partial T}{\partial z}) \tag{3.8}$$

$$\varphi = 2\ \mu[(\frac{\partial u}{\partial x})^2 + \left(\frac{\partial v}{\partial y}\right)^2 + (\frac{\partial w}{\partial z})^2 + \frac{1}{2}(\frac{\partial v}{\partial x} + \frac{\partial u}{\partial y})^2 + \frac{1}{2}\ (\frac{\partial w}{\partial y} + \frac{\partial v}{\partial z})^2 + \frac{1}{2}\ (\frac{\partial u}{\partial z} + \frac{\partial w}{\partial x})^2 \tag{3.9}$$

Also, for nanofluids.

$$\nabla\left(\rho_{nf}\bar{V}C_{p,nf}\bar{T}\right) = \left(k_{nf}\ grad\ (\bar{T}) - \rho_{nf}\overline{T'}C_{p,nf}\overline{V'}\right) \tag{3.10}$$

where, k_{nf} is the effective thermal conductivity and $C_{p,nf}$ is the effective specific heat of the nanofluid.

3.2 NUMERICAL MODELLING

In the numerical section, computational fluid dynamics (CFD) is used to simulate the conduct of nanofluids inside pipe flow with fins. CFD gives an effective device for studying complicated fluid dynamics problems, making an allowance for specified research and optimization of go with the drift dynamics. Through numerical simulations, the effect of diverse parameters consisting of nanoparticle concentration, fin properties, and pipe geometry can be evaluated on thermal performance.

Key components of the numerical analysis include:

- Mesh generation and discretization of the computational domain.
- Solution of the governing equations using iterative methods.
- Validation of numerical results through comparison with experimental data or analytical solutions.

By utilizing CFD techniques, optimization of heat transfer efficiency and investigation of the potential of nanofluids in improving heat transfer performance can be accomplished. This chapter provides an essential basis for the upcoming numerical studies discussed in the thesis.

Geometry Creation: The first step is to create a 3D model of the pipe, including the flow domain and internal structures, such as nano-particle distributions or any internal features that influence fluid flow. The geometry should accurately represent the flow channels, boundaries, and any areas where the fluid interacts with the surface.

Mesh Generation: Once the geometry is created, it needs to be discretized into small computational elements or cells. This process is known as mesh generation. The quality of the mesh is crucial for ensuring accurate CFD simulations, especially in regions with complex flow patterns or near walls where the nanofluid interacts with surfaces.

Boundary Conditions: The necessary boundary conditions for the simulation, including inlet velocity, temperature, pressure, and any other relevant parameters specific to the nanofluid flow are defined. These boundary conditions are essential for ensuring the correct representation of the system, particularly the interactions between the nanoparticles and the fluid.

Solver Setup: Configuration of the CFD solver settings, adjusting solution methods, convergence criteria, and numerical schemes according to the flow characteristics, turbulence model, and available computational resources are done. The solver settings must be selected carefully to align with the type of fluid, flow regime, and computational capacity.

Simulation Run: CFD simulation are run using the predefined geometry, mesh, boundary conditions, turbulence model, and solver settings. Depending on the complexity of the simulation and available computational resources, the run time can vary from several hours to several days.

Post-processing: After the simulation is complete, results are analysed. This includes visualizing flow patterns, temperature distributions, pressure drops, heat transfer rates, and the effects of nanoparticles on the fluid. Post-processing tools are essential for extracting valuable insights from the simulation data.

Validation and Verification: CFD results are validated by comparing them with experimental data or analytical solutions available in the literature. Validation ensures that the simulation accurately represents the physical system, while verification confirms that the results are consistent with theoretical expectations and physical principles.

Optimization and Design Iteration: CFD results are used to optimize the internal design or operating conditions of the pipe. This may involve adjusting parameters such as flow rates, nanofluid concentrations, or internal features to improve performance or efficiency.

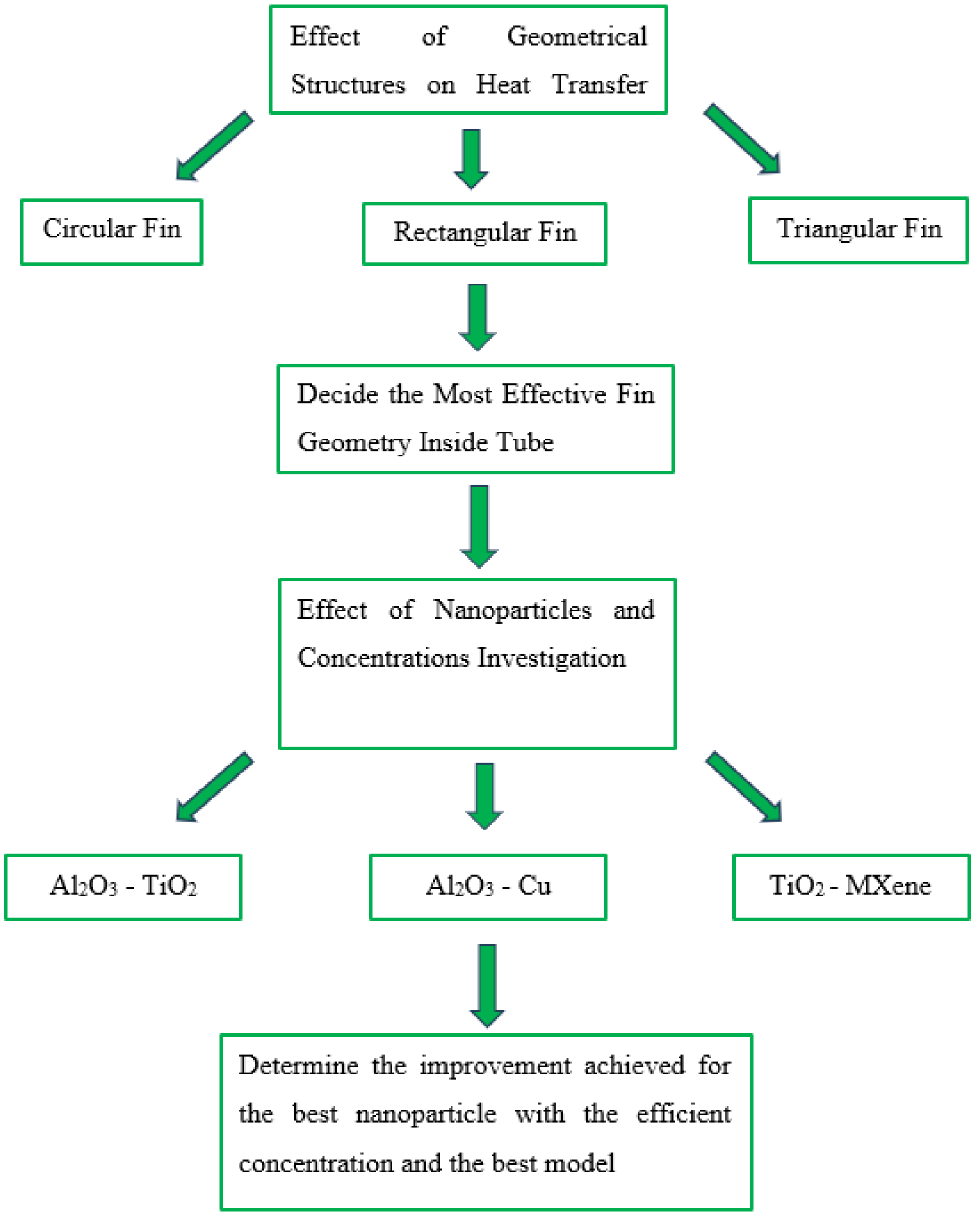

Figure 3: Thesis workflow diagram

3.3 PHYSICAL MODEL

This section explains the numerical analysis carried out in the current study. ANSYS Fluent simulation are used to solve the governing equations defining steady, laminar flow and heat transfer in a tube with different extended geometries and nanofluid as the working fluid, as reported in the previous section. The physical model of the system was rigorously developed using ANSYS Design Modeler, with geometric dimensions that corresponded to the measurements. Specifications of the physical model can be seen in Table 2.

Table 2: Specifications of the physical model

Data	
Inner diameter of the pipe (D)	0.022 m
Length of the pipe (L)	2.2 m
Inlet temperature (T_{inlet})	293 K
Reynolds number (Re)	Varies between 800 and 2000

For each of the three geometries, fin lengths (L) of 4 mm, 6 mm, 8 mm, and 10 mm were analyzed, and the best results were observed with the triangle fin geometry at L = 10 mm. Following this, the effect of varying the fin height (a) on the thermal performance of the nanofluid was studied, using the optimal L and triangle geometry. The analysis of the effects of fin geometry, L, and a provides a comprehensive understanding of the most effective parameters for enhancing heat transfer performance in nanofluid flow applications.

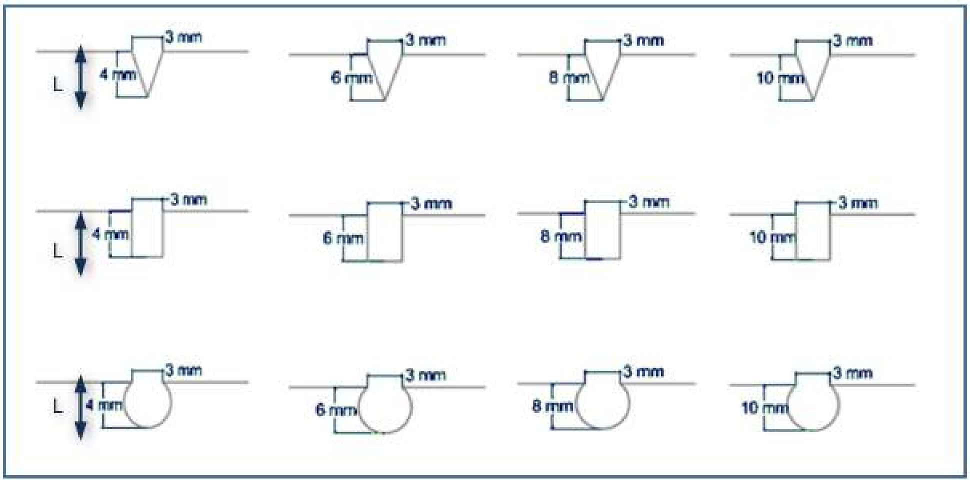

Figure 4: Fin structures with different geometries and sizes

3.4 MESH GENERATIONS AND MESH INDEPENDENCE

In computational simulations, the mesh size has a significant impact on the accuracy and convergence of the results. As the mesh resolution increases, the solution becomes more refined, but this also leads to higher computational costs. Therefore, during the modeling process, the mesh size should be increased until a mesh-independent solution is achieved. A mesh-independent result is one where further refinement of the mesh no longer significantly affects the outcome, ensuring that the simulation results are reliable and accurate. Additionally, in turbulent flows, care should be taken to ensure that the y+ values do not exceed the reference values when meshing near the boundaries. To achieve this, a finer mesh is applied in the regions close to the boundaries. This approach helps to balance computational efficiency with the precision of the analysis, ensuring that the results obtained are not influenced by the chosen mesh resolution.

Table 3: Mesh independence study table

Re (1200)	Element Number	Nusselt Number	Error Numerical/Langhaars (%)
1	12000	10.80	3.70
2	25000	10.72	2.99
3	35000	10.44	0.38
4	50000	10.46	0.57
5	63500	10.48	0.76
6	100000	10.47	0.67

As a result of the mesh study, the element number that ranked 3rd in terms of having the lowest error margin and the closest numerical correlation to Langhaar's correlation was observed. This element number corresponds to a mesh with 35,000 elements, and the analyses were conducted as previously stated using a 2D simulation. It was also observed that similar close approximations were achieved with subsequent element counts, and based on this approach, the most effective element count was determined to be the mesh with 35,000 elements.

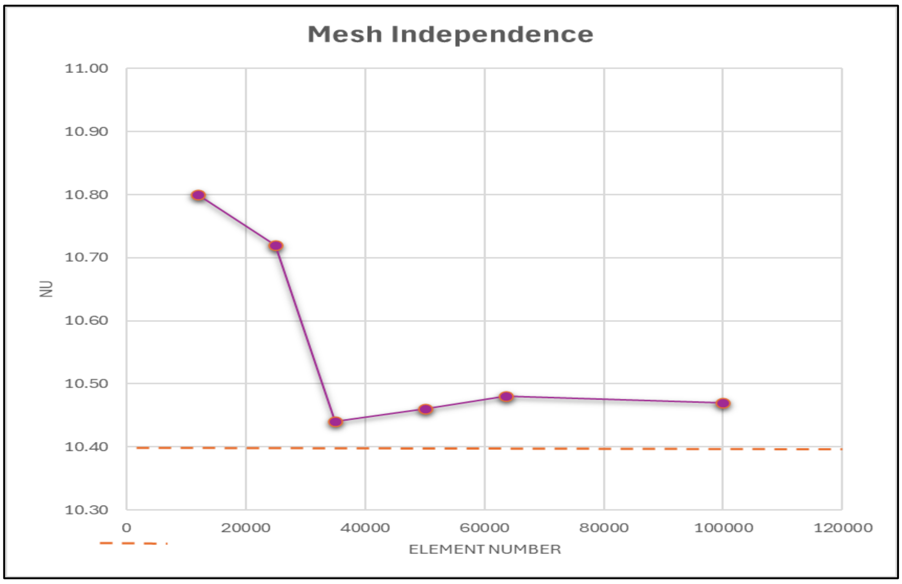

Figure 5: Variation of Nusselt number with different mesh structure for tube

3.5 BOUNDARY CONDITIONS

To solve the nonlinear partial differential equations mentioned in the previous chapters, it is necessary to accurately define the boundary conditions related to the physical problem under consideration. In this study, Reynolds number is defined within the range of 800 to 2000. Additionally, the tube outlet pressure is set as a constant 0 Pa, and the tube inlet temperature is defined as 298.15 K.

The thermophysical properties of water and mixed nanoparticles, namely Al_2O_3, Al_2O_3-Cu, and MXene, are determined based on our calculations. These calculations indicate that water mixed with these three nanoparticles exhibits new thermophysical properties, which remained constant throughout the flow. A uniform heat flux of 5725 W/m^2 is applied across the entire surface of the tube.[76]

Table 4: Boundary conditions for calculations and numerical analysis

Boundary	Type	Parameters
Tube Inlet	Reynolds Number	800-2000
Tube Inlet	Temperature	298.15 K
Tube Surface	Uniform Heat Flux	5725 W/m^2
Tube Outlet	Pressure Outlet	0 Pa

The system setup was developed based on the parameters listed in this table, and the analysis was conducted using the ANSYS CFD simulation software. Detailed validation procedures and results are provided in the validation section. Based on the literature review, the thermophysical properties of water and nanoparticles are presented in the following table.

Table 5: Thermophysical properties of base fluid and nanoparticles

Thermophysical Properties	Water	Al_2O_3	TiO_2	Cu	MXene
Density (kg/m^3)	996.5	3970	4175	8933	4520
Specific Heat (J.kg^{-1}K)	4181	765	692	385	606
Viscosity μ (Pa.s)	0.001	-	-	-	-
Thermal Conductivity (W.m−1.K)	0.613	40	8.4	400	268.4

The thermophysical property equations were utilized to determine the characteristics of each nanoparticle-water mixture at different concentrations. The thermophysical properties of Water-Al_2O_3-TiO_2 nanofluid were calculated using the previously provided formulas and corresponding concentrations. The table below presents the nanofluid properties (Water-Al_2O_3-TiO_2) for each concentration level. [77]

Table 6: Water- Al_2O_3 - TiO_2Thermophysical properties, nanofluid at different nanoparticle volume concentrations

Al_2O_3	**TiO_2**	**(Al_2O_3 - TiO_2)**	**Thermo-Physical Properties of Nanofluid**			
Volume Fraction %	Volume Fraction %	Total Volume Fraction %	Density of Nanofluid (kg/m^3)	Specific Heat ($J.kg^{-1}.K$)	Viscosity μ (Pa.s)	Thermal Conductivity ($W.m^{-1}.K$)
2.5	1.5	4	1118.5	3682.5	0.0034	0.68
5	3	8	1240.5	3282.1	0.0056	0.76
10	6	16	1484.6	2678.8	0.0120	0.92
3	5	8	1244.6	3268.9	0.0042	0.75

The properties of the nanofluid (Water, Al_2O_3, Cu) at different concentrations are provided in the table below. [78]

Table 7: Thermophysical properties of Water- Al_2O_3 - Cu nanofluid at different nanoparticle volume concentrations at 298.15 K

Al_2O_3	**Cu**	**(Al_2O_3 – Cu)**	**Thermo-Physical Properties of Nanofluid**			
Volume Fraction %	Volume Fraction %	Total Volume Fraction %	Density of Nanofluid (kg/m^3)	Specific Heat ($J.kg^{-1}.K$)	Viscosity μ (Pa.s)	Thermal Conductivity ($W.m^{-1}.K$)
2.5	1.5	4	1189.9	3468.6	0.0034	0.69
5	3	8	1383.3	2955.4	0.0054	0.77
10	6	16	1770.0	2265.4	0.0114	0.95
3	5	8	1482.5	2762.9	0.0038	0.77

Additionally, a new nanofluid (Water-TiO_2-MXene) is studied and the properties at various concentrations are presented in the table below.[78]

Table 8: Thermophysical properties of Water- TiO_2-MXene nanofluid at different nanoparticle volume concentrations at 298.15 K

$\mathbf{TiO_2}$	**MXene**	**($\mathbf{TiO_2}$-MXene)**	**Thermo-Physical Properties of Nanofluid**			
Volume Fraction %	Volume Fraction %	Total Volume Fraction %	Density of Nanofluid (kg/m^3)	Specific Heat ($J.kg^{-1}.K$)	Viscosity μ (Pa.s)	Thermal Conductivity ($W.m^{-1}.K$)
2.5	1.5	4	1128.8	3643.7	0.0022	0.68
5	3	8	1261.1	3219.1	0.0026	0.75
10	6	16	1525.8	2590.8	0.0038	0.91
3	5	8	1268.0	3199.2	0.0024	0.76

3.6 VALIDATION OF THE MODEL

In this section, a detailed review of research on the mathematical modeling of hydrodynamic and thermally developing flow is presented based on the methods for calculation under constant heat input condition [73]. Calculation methods for Constant Heat Input (Parabolic Velocity Profile) and Constant Heat Input (Langhaar's Velocity Profile) are discussed. Nusselt number calculations are performed, and the importance of these calculations is emphasized. A detailed analysis of the Reynolds number and non-fully developed flow is conducted, and the fully developed state is examined as a function of pipe length. The pipe length in the analysis is 2.2 meters, with investigations extending to 8 meters. It is observed that at a pipe length of 8 meters, the flow transitions to a fully developed state.

3.6.1 Constant Heat Input (Parabolic Velocity Profile)

The shape of the velocity profile in fluid flow, especially in laminar flow, is crucial for understanding heat transfer and fluid dynamics, particularly under constant heat input conditions. In this profile, the maximum velocity occurs at the center and decreases towards the walls, affecting the temperature gradient and convective heat transfer. This profile is commonly observed in cylindrical pipes and channels, where a constant heat source influences the behavior of the fluid. Maximizing heat transfer efficiency is essential for advanced thermal management and system design in industrial environments such as heat exchangers and cooling systems [75].

$$Nu = 4.36 + \frac{0.023(RePr/(\frac{x}{d})}{1+0.0012(RePr/(\frac{x}{d})^{0.8})} \tag{3.10}$$

3.6.1.1 Constant heat input (Langhaar's Velocity Profile)

Langhaar's velocity profile serves as a crucial theoretical model for understanding the velocity distribution and temperature profiles of a fluid under constant heat input conditions. This model is particularly prevalent in studies involving laminar flow and heat transfer. When exposed to continuous heat input, the relationship between fluid velocity and temperature distribution becomes significant in understanding heat conduction and convection within the system. Langhaar's profile plays a vital role in enhancing heat transfer efficiency and facilitating convective processes in various industrial applications, including heaters, cooling systems, and pipelines. Consequently, Langhaar's velocity profile is regarded as a fundamental tool in the design of heat transfer and thermal management systems [75].

$$Nu = 4.36 + \frac{0.036(RePr/(\frac{x}{d})}{1+0.0012(RePr/(\frac{x}{d})^{0.8})} \tag{3.11}$$

3.6.2 Validation of Constant Heat Input using Langhaar's Velocity Profile

This study aims to construct a theoretical model capable of reliably predicting heat transfer in a defined region under the condition of a constant heat input. To validate the model, the effects of a steady heat flux on temperature and velocity distributions were analyzed. The analysis employs nonlinear partial differential equations that describe the behavior of incompressible fluid flow and heat transfer. Variations in temperature and velocity within the boundary layer were evaluated at different distances from the central axis for standard fluids, and the findings were compared with results derived from numerical integration and fourth-order methods to ensure accuracy.

Table 9: Comparison table of theoretical and numerical results based on Nusselt numbers

Nusselt Number	Numerical Result	Theoretical Results
800	8.65	8.5
1200	10.44	10.4
1600	13.5	12.2
2000	14.6	13.9

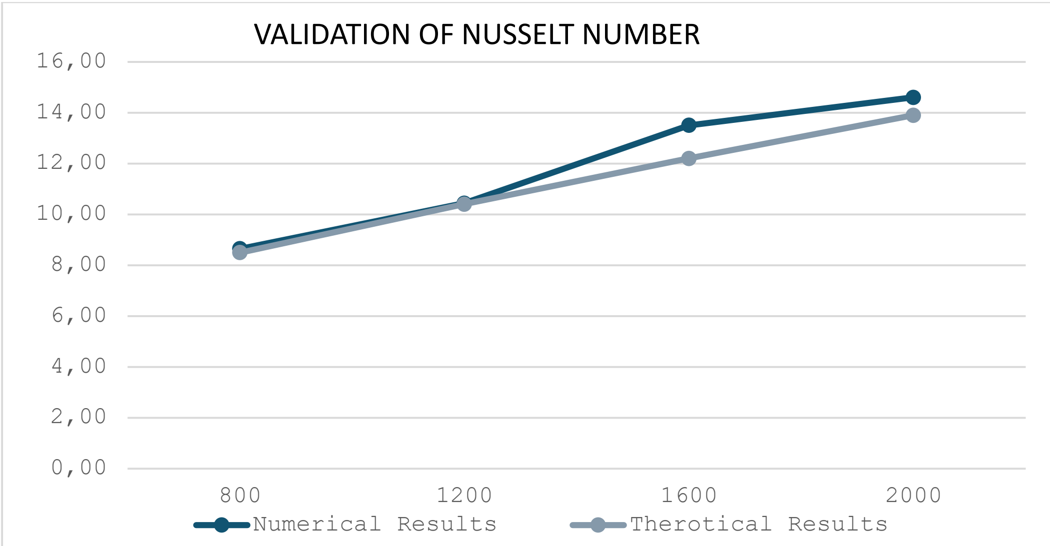

Figure 6: Validation study of Nusselt number

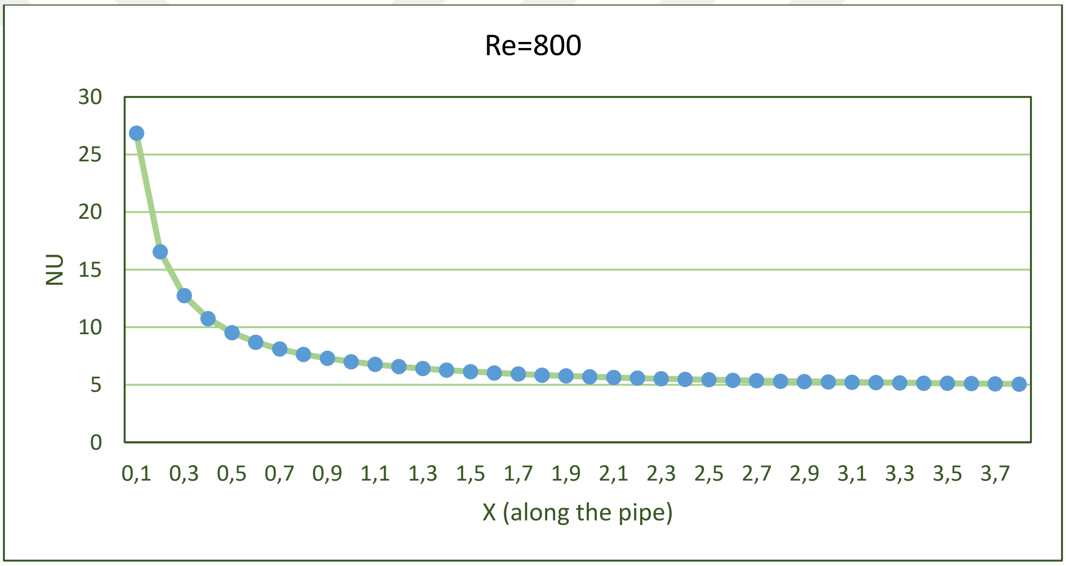

Figure 7: According to the Re: 800 - constant heat input (Langhaar's velocity profile) vs Nusselt number

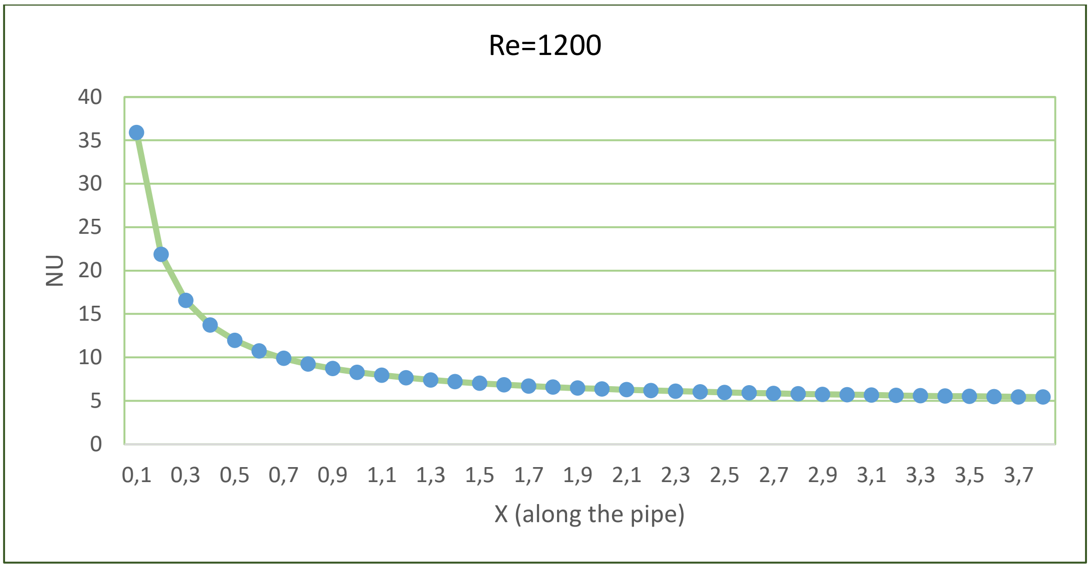

Figure 8: According to the Re: 1200 - Constant heat input (Langhaar's velocity profile) vs Nusselt number

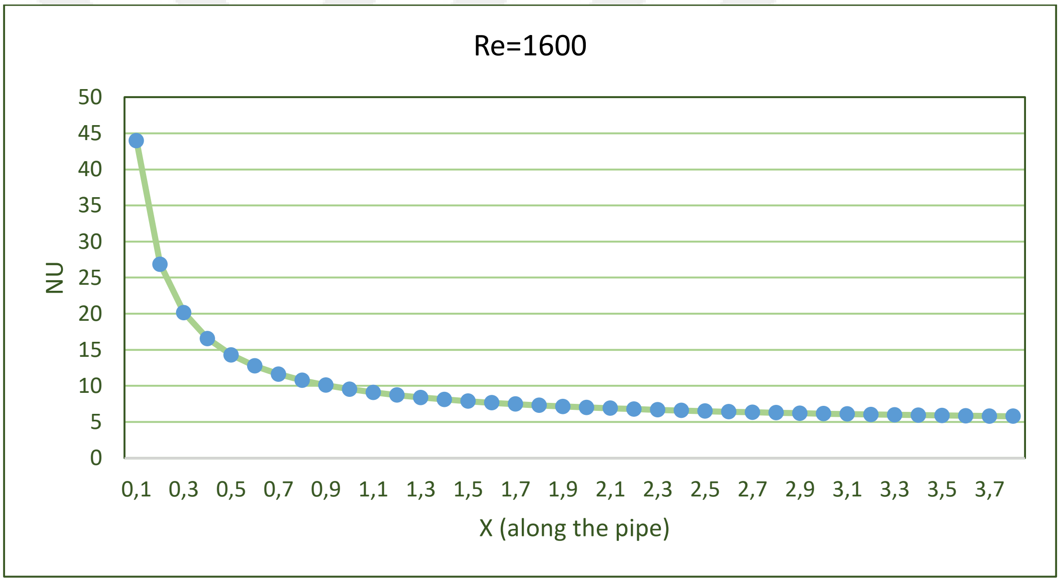

Figure 9: According to the Re: 1600 - constant heat input (Langhaar's velocity profile) vs Nusselt number

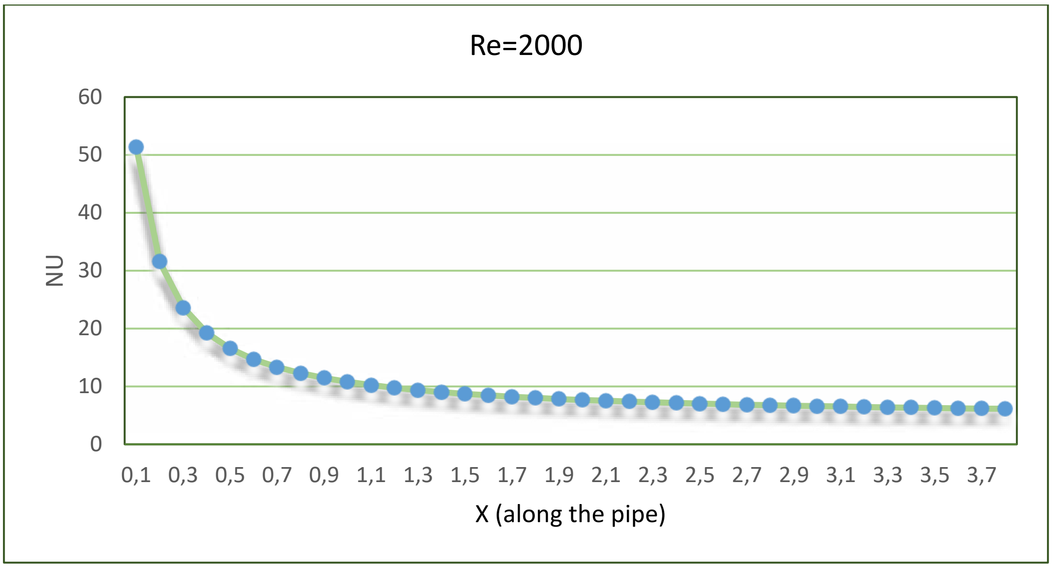

Figure 10: According to the Re: 2000 - constant heat input (Langhaar's velocity profile) vs Nusselt number

3.7 TEST MATRIX

In the scope of the studies, 80 cases with water and concentrations of different nanofluids are simulated.

In the analysis, firstly the effect of geometry was examined. The most efficient geometry and nanofluids at different concentrations were examined. As a result of the analysis, the best fin structure and the best nanofluid concentration were observed and the conclusion was reached. As can be seen in Table, analyses were run according to nanofluids and different geometry fins in the pipe.

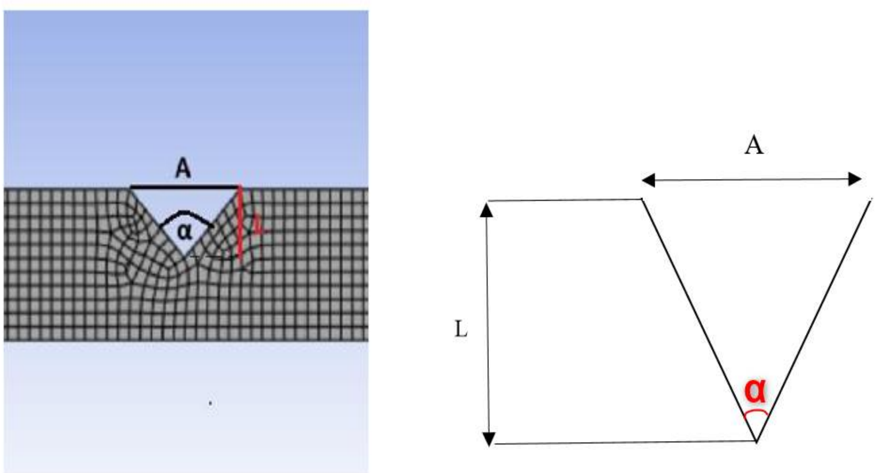

Figure 11: triangle geometric, length and angle view

Table 10: Test matrix of simulations

CASE	Geometries	A & L (mm / degrees)	Water / Nanofluid	Volume fraction %	Reynolds Number
1	triangle	A=3 mm, L=4 mm	Water	-	800,1200,1600,2000
2	triangle	A=3 mm, L=6 mm	Water	-	800,1200,1600,2000
3	triangle	A=3 mm, L=8 mm	Water	-	800,1200,1600,2000
4	triangle	A=3 mm, L=10 mm	Water	-	800,1200,1600,2000
5	Rectangular	A=3 mm, L=4 mm	Water	-	800,1200,1600,2000
6	Rectangular	A=3 mm, L=6 mm	Water	-	800,1200,1600,2000
7	Rectangular	A=3 mm, L=8 mm	Water	-	800,1200,1600,2000
8	Rectangular	A=3 mm, L=10 mm	Water	-	800,1200,1600,2000
9	Circle	A=3 mm, L=4 mm	Water	-	800,1200,1600,2000
10	Circle	A=3 mm, L=6 mm	Water	-	800,1200,1600,2000
11	Circle	A=3 mm, L=8 mm	Water	-	800,1200,1600,2000
12	Circle	A=3 mm, L=10 mm	Water	-	800,1200,1600,2000
13	triangle	A=60 degrees, L=10 mm	Water	-	800,1200,1600,2000
14	triangle	A=41 degrees, L=10 mm	Water	-	800,1200,1600,2000
15	triangle	A=29 degrees, L=10 mm	Water	-	800,1200,1600,2000
16	triangle	A=17 degrees, L=10 mm	Water	-	800,1200,1600,2000

Table 10 Cont.

16-20	triangle	A=17 degrees, L=10 mm	Water-Al_2O_3/TiO_2	2.5-1.5	800,1200,1600,2000
21-24	triangle	A=17 degrees, L=10 mm	Water-Al_2O_3/TiO_2	5-3	800,1200,1600,2000
25-28	triangle	A=17 degrees, L=10 mm	Water-Al_2O_3/TiO_2	10-6	800,1200,1600,2000
29-32	triangle	A=17 degrees, L=10 mm	Water-Al_2O_3/TiO_2	3-5	800,1200,1600,2000
33-36	triangle	A=17 degrees, L=10 mm	Water-Al_2O_3/Cu	2.5-1.5	800,1200,1600,2000
37-40	triangle	A=17 degrees, L=10 mm	Water-Al_2O_3/Cu	5-3	800,1200,1600,2000
41-44	triangle	A=17 degrees, L=10 mm	Water-Al_2O_3/Cu	10-6	800,1200,1600,2000
45-48	triangle	A=17 degrees, L=10 mm	Water-Al_2O_3/Cu	3-5	800,1200,1600,2000
49-52	triangle	A=17 degrees, L=10 mm	Water-TiO_2/ MXene	2.5-1.5	800,1200,1600,2000
53-56	triangle	A=17 degrees, L=10 mm	Water-TiO_2/MXene	5-3	800,1200,1600,2000
57-60	triangle	A=17 degrees, L=10 mm	Water-TiO_2/ MXene	10-6	800,1200,1600,2000
61-64	triangle	A=17 degrees, L=10 mm	Water-TiO_2/ MXene	3-5	800,1200,1600,2000
65-68	triangle	A=17 degrees, L=10 mm	Water-Al_2O_3/ TiO_2	2.5-1.5	800,1200,1600,2000
69-72	triangle	A=17 degrees, L=10 mm	Water-Al_2O_3/ TiO_2	5-3	800,1200,1600,2000
73-76	triangle	A=17 degrees, L=10 mm	Water-Al_2O_3/ TiO_2	10-6	800,1200,1600,2000
77- 80	triangle	A=17 degrees, L=10 mm	Water-Al_2O_3/ TiO_2	3-5	800,1200,1600,2000

CHAPTER IV
RESULTS AND DISCUSSIONS

In this section, after the methodology and problem definition, the effects of nanoparticles and geometric structures on heat transfer are investigated. First, studies are conducted for 3 different types of geometry, and the effect of geometry was examined. In the meantime, water was preferred as fluid. Then, the effect of nanoparticles is discussed according to thermophysical calculations with certain formulas according to the best geometry is selected. For this purpose, thermophysical calculations were made for each type of nanoparticle, and the results are presented in graphs. It assumed that the fluid is single-phase. The nanoparticles examined were Al_2O_3-TiO_2; Al_2O_3-Cu; and TiO_2-MXene mixed at different concentrations. Nanofluid calculations on the best selected geometry is performed using ANSYS 2024R2. The most effective geometric structure is determined through graphs and simulations. Then, nanofluids with different concentration levels are analyzed, and the structure providing the best heat transfer is determined, and the most effective nanofluid and geometry are selected through graphs and simulations.

4.1 EFFECT OF FINS HEIGHT ON HEAT TRANSFER AND NUSSELT NUMBER IN PIPE FLOW: THEROTICAL AND NUMERICAL INVESTIGATION

After completing the validation process, the heat transfer performance of triangular, circular, and rectangular shaped fins placed inside the pipe was analyzed with a particular focus on nanofluid flow. The results demonstrated that the inclusion of fins significantly enhances heat transfer within the pipe by disrupting the thermal boundary layer and increasing turbulence. Among the tested geometries, triangular fins exhibited superior heat transfer performance compared to semi-circular and square fins, primarily due to their streamlined shape, which minimizes flow resistance while maximizing surface area. Detailed findings are presented below in graphs and tables, providing a comparative analysis of each fin type's influence on heat transfer efficiency. Using ANSYS Fluent simulations, three distinct fin geometries “triangular, rectangular, and circular” were analyzed inside a pipe. The research began by provides exploring the impact of fin length (L) on heat transfer, followed by an examination of the fin height (A) to identify the optimal parameters. The pipe length was fixed at 2200 mm, and its diameter was 22 mm. The changes in Nusselt numbers have been analyzed based on the shapes shown above, and it has been observed that the triangular shape better results. Below, the analysis results in the form of tables and graphs are presented for triangular, rectangular, and circular shape fins according to the lengths (L) and constant width (A) which was 3 mm.

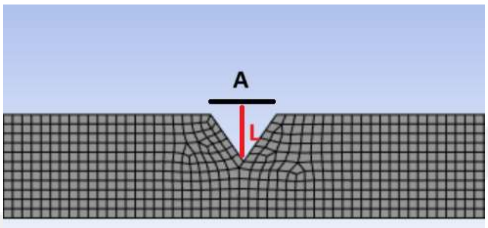

Figure 12: Representation of Length (L) and A (Width) of fin

4.1.1 Effects of Triangular Fins on Heat Transfer Enhancement

For the water flow in pipe, the triangular fin structure was placed in a 2200 mm long pipe at equal intervals (10 pieces) analysis are done for 4 different Reynolds numbers. The width of these triangles was kept constant in each analysis, and analyses were run in 4 different lengths (L). According to the results it was determined that the flow area narrowed with an increase in the triangle length, and due to this narrowing, the vortex structure formation inside the tube was seen more, which accelerated the laminar fluid by acting as a turbulator, and there was a serious increase in heat transfer enhancement. The CFD simulations were run as 2-D, and the best system structure was determined as a result of 16 different analyses. The heat transfer coefficient was found for each length value (L=4, 6, 8, 10 mm) results are given in 4 different tables below, and the best Nusselt number was found with the help of the convection formula. Accordingly, the best length (L) was determined for the triangular fin structure. The found Nusselt numbers and heat transfer coefficient values are given in Table 11 to 14.

Table 11: Nusselt number and heat transfer coefficients at triangle L=4

Triangle L=4		
Reynolds Number	**Nusselt Number**	**h**
800	11,6	263,2
1200	17,0	437,0
1600	21,8	568,0
2000	25,5	667,7

Table 12: Nusselt number and heat transfer coefficients at triangle L=6

triangle L=6		
Reynolds Number	**Nusselt Number**	**h**
800	13,0	348,5
1200	19,3	500,0
1600	23,6	607,7
2000	26,6	697,4

Table 13: Nusselt number and heat transfer coefficients at triangle L=8

triangle L=8		
Reynolds Number	**Nusselt Number**	**h**
800	14,8	360,5
1200	22,2	468,7
1600	26,5	587,3
2000	28,9	698,9

Table 14: Nusselt number and heat transfer coefficients at triangle L=10

triangle L=10		
Reynolds Number	**Nusselt Number**	**h**
800	16,3	409,2
1200	25,6	726,0
1600	29,9	761,1
2000	30,5	831,8

As can be seen from Tables 11 to 14, an increase in both Nusselt number and heat transfer coefficients was observed as height increased. In addition, when the velocity of fluid increases, the turbulator speed increases for the vortex formed, and a higher tendency was realized at Re = 2000. As a result, it was observed that the best fin model for the Triangular fins is 10 mm length for Re = 2000.

4.1.2 Effects of Rectangular Fins on Heat Transfer Enhancement

For the water flow in pipe, the rectangular fin structure was placed in a 2200 mm long pipe at equal intervals (10 pieces) analysis are done for 4 different Reynolds numbers. The width of these rectangular was kept constant in each analysis, and analyses were run in 4 different lengths (L). According to the results, it was determined that the flow area narrowed with the increase in the rectangular length, and due to this narrowing, the vortex structure formation inside the tube was seen more, which accelerated the laminar fluid of the geometry in the system by acting as a turbulator, and there was a serious increase in heat transfer enhancement. The CFD simulations were run as 2-D, and the best system structure was determined according to 16 different analyses. The heat transfer coefficient was found for each length value (L=4, 6, 8, 10 mm) results are given in 4 different tables below, and the best Nusselt number was found with the help of the convection formula. Accordingly, the best length (L) was determined for the rectangular fin structure. The found Nusselt numbers and heat transfer coefficient values are given in Table 15 to 18.

Table 15: Nusselt number and heat transfer coefficients at rectangular L=4

Rectangular L=4		
Reynolds Number	**Nusselt Number**	**H**
800	10,5	244,1
1200	15,8	431,8
1600	20,6	560,9
2000	24,2	659,6

Table 16: Nusselt number and heat transfer coefficients at rectangular L=6

Rectangular L=6		
Reynolds Number	**Nusselt Number**	**h**
800	12,0	328,0
1200	17,9	488,8
1600	22,5	613,8
2000	25,7	701,2

Table 17: Nusselt number and heat transfer coefficients at rectangular L=8

Rectangular L=8		
Reynolds Number	**Nusselt Number**	**h**
800	14,0	382,7
1200	19,8	539,1
1600	24,0	654,0
2000	27,0	736,3

Table 18: Nusselt number and heat transfer coefficients at rectangular L=10

Rectangular L=10		
Reynolds Number	**Nusselt Number**	**h**
800	15,5	422,2
1200	21,0	574,1
1600	25,0	682,3
2000	28,1	765,6

As can be seen from Tables 15 to 18 an increase in both Nusselt number and heat transfer coefficients was observed as height increased. In addition, when the velocity of fluid increases, the turbulator speed increases for the vortex formed, and a higher tendency was realized at Re = 2000. As a result, it was observed that the best fin model for the rectangular fins is 10 mm for Re = 2000.

4.1.3 Effects of Circular Fins on Heat Transfer Enhancement

For the water pipe flow, the circular fin structure was placed in a 2200 mm long pipe at equal intervals (10 pieces) analysis are done for 4 different Reynolds numbers. The width of these circulars was kept constant in each analysis, and analyses were run in 4 different lengths (L). According to the results, it was determined that the flow area narrowed with the increase in the circular length, and due to this narrowing, the vortex structure formation inside the tube was seen more, which accelerated the laminar fluid by acting as a turbulator, and there was a serious increase in heat transfer enhancement. The CFD simulations were run as 2-D, and the best system structure was determined according to 16 different analyses. The heat transfer coefficient was found for each length value (L=4, 6, 8, 10 mm) results are given in 4 different tables below, and the best Nusselt number was found with the help of the convection formula. Accordingly, the best length (L) was determined for the circular fin structure. The found Nusselt numbers and heat transfer coefficient values are given in Table 19 to 22.

Table 19: Nusselt number and heat transfer coefficients at circle L=4

Circle L=4		
Reynolds Number	**Nusselt Number**	**h**
800	9,5	259,5
1200	14,0	381,0
1600	18,5	505,8
2000	22,3	608,6

Table 20: Nusselt number and heat transfer coefficients at circle L=6

Circle L=6		
Reynolds Number	**Nusselt Number**	**h**
800	10,2	278,8
1200	15,3	417,9
1600	20,2	551,4
2000	24,0	655,4

Table 21: Nusselt number and heat transfer coefficients at circle L=8

Circle L=8		
Reynolds Number	**Nusselt Number**	**h**
800	11,5	313,0
1200	16,9	462,1
1600	21,8	594,5
2000	25,4	692,3

Table 22: Nusselt number and heat transfer coefficients at circle L=10

Circle L=10		
Reynolds Number	**Nusselt Number**	**h**
800	12,7	345,9
1200	18,2	496,4
1600	23,0	628,0
2000	26,5	772,0

As can be seen from Tables 19 to 22 an increase in both Nusselt number and heat transfer coefficients was observed as height increased. In addition, when the velocity of fluid increases, the turbulator speed increases for the vortex formed, and a higher tendency was realized at Re = 2000. As a result, it was observed that the best fin model for the Circular fins is 10 mm length for Re = 2000.

4.2 COMPARISONS EFFECTS OF FINS ON HEAT TRANSFER AND NUSSELT NUMBER IN PIPE FLOW AFTER

Different types of fin structures in each shape, namely Triangular, Rectangular and Circular, were placed at equal intervals on the 2200 mm long pipe. As stated in the above section, each of them was analyzed separately with different lengths and with velocities between Re=800 and 2000, which is the Laminar flow regime, accompanied by water fluid. Detailed results of the analysis, for each shape are given in the previous section. With the help of simulations, the following graphs were created for each Reynolds number according to length change and shape effect.

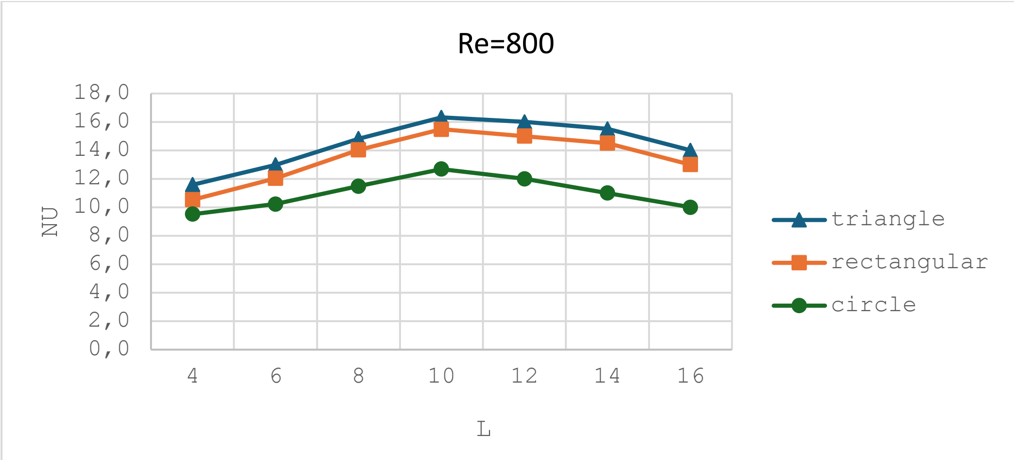

Figure 13: Variations in Nusselt number for triangular, rectangular, and circular fins shape based on changes in L values at Reynolds number of 800

When the results are examined, it is seen that the triangular and rectangular fin structures exhibit a similar structure, but the effect of the circular fin on heat transfer is not as effective as the triangular and rectangular fin structures. The reason for this can be explained as the narrowing of the flow area hitting the fin surface does not have as much effect as other structures in changing the movement area of the liquid fluid compared to other shapes.

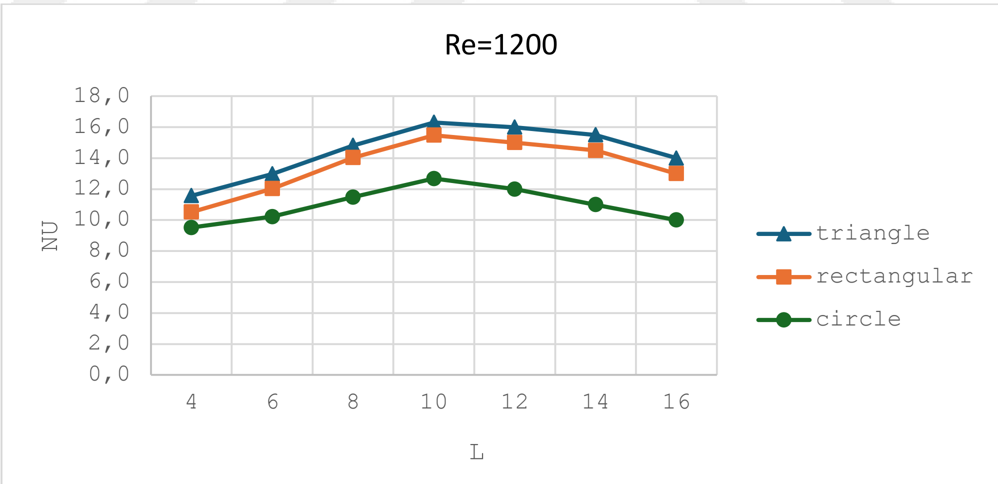

Figure 14: Variations in Nusselt number for triangle, square, and semicircle shapes based on changes in L values at a Reynolds number of 1200

Looking at Figure 14, the same trend is observed at Re=1200 and the effect of the triangular fin structure on heat transfer is observed to be better than other fin structures.

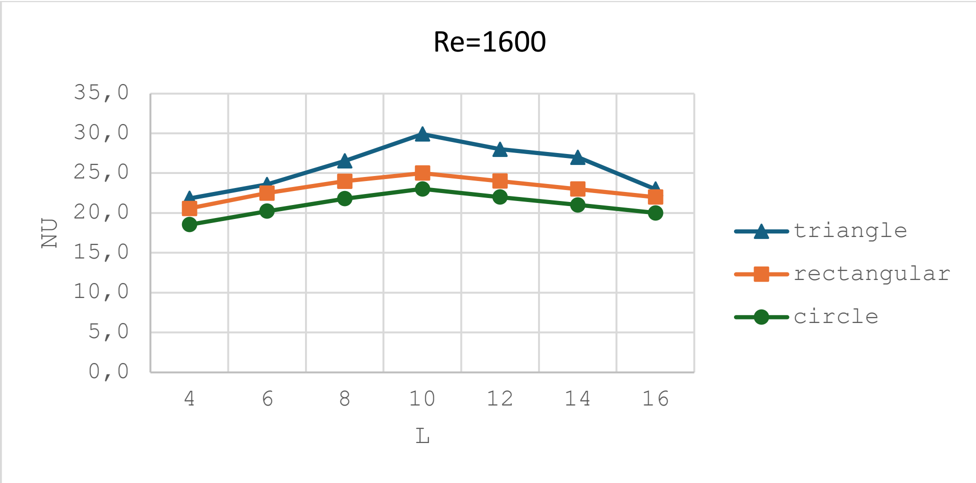

Figure 15: Variations in Nusselt number for triangle, square, and semicircle shapes based on changes in L values at a Reynolds number of 1600

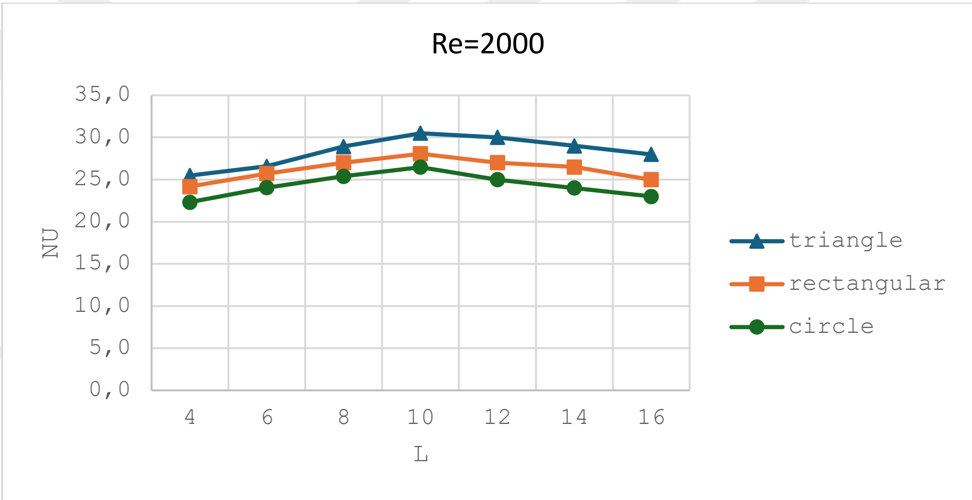

Figure 16: Variations in Nusselt number for triangle, square, and semicircle shapes based on changes in L values at a Reynolds number of 2000.

When the analyses were performed at other Reynolds numbers, as can be seen in Figures 13 to 16, when the effect of length change was examined, the effect of the fluid on heat transfer was mostly seen in the form of a triangular fin.

Also, the Friction factor is the most important criterion for selecting structure of fins because if the friction factor is high, it means that the tube creates an adverse effect on the flow in the system and this has a negative effect on the movement of the fluid in the system. A high friction factor is a disadvantage for the system. So, this study also checks the system friction factor and compare the 3 different fin structures friction factors can be seen in Figure 17.

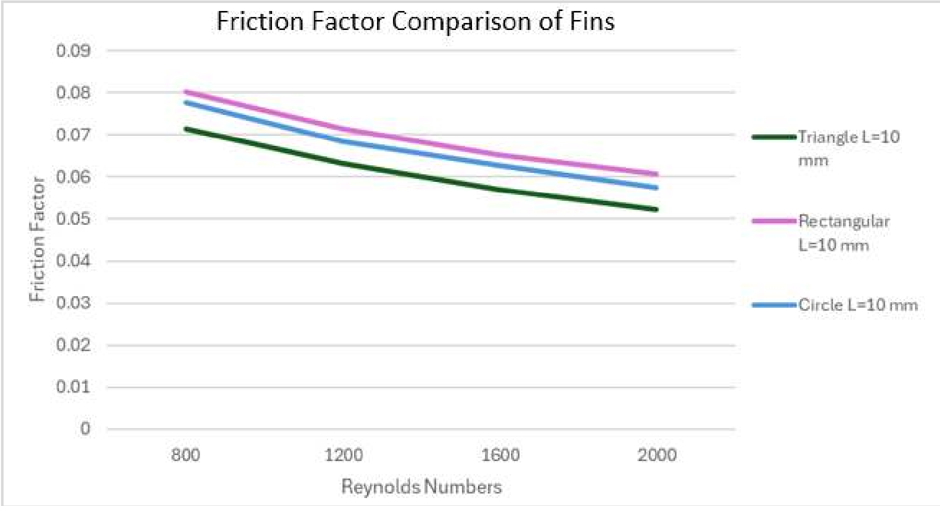

Figure 17: Friction factor comparison of Fins for Reynolds Number 800 to 2000

As seen in Figure 17, when the fins with the highest nusselt number are compared among the fin structures, the geometry with both the high nusselt number and the lower effect of the friction factor appears to be the Triangular fin structure. This shows that the triangular fin structure has a lower negative effect of the friction factor study.

For this reason, the triangular fin was selected for the angle change study, which is another geometric analysis. Before examining the angle change effect, it is necessary to make a comparison within the triangular fin structure. Within the examined lengths of the Triangular Fins, L = 4,6,8,10 mm. It was performed with the Performance Evaluation Criteria, which has a formulation including the friction factor value obtained with the help of ANSYS software and the Nusselt number calculated with the help of the obtained values. Because the geometry of a system significantly impacts its thermal characteristics and heat transfer performance. This effect is particularly critical in systems employing passive methods, where geometric configuration plays a crucial role. Therefore, in this study, the previously validated passive method system with fins was analyzed to investigate the influence of geometric modifications. Changes were made to the fin structures, and the Nusselt number, heat transfer coefficient, and friction factor were evaluated. Based on these evaluations, the optimal model was identified. Graphics regarding the previously mentioned PEC formulation which was used to determine this model can be seen in figure below.

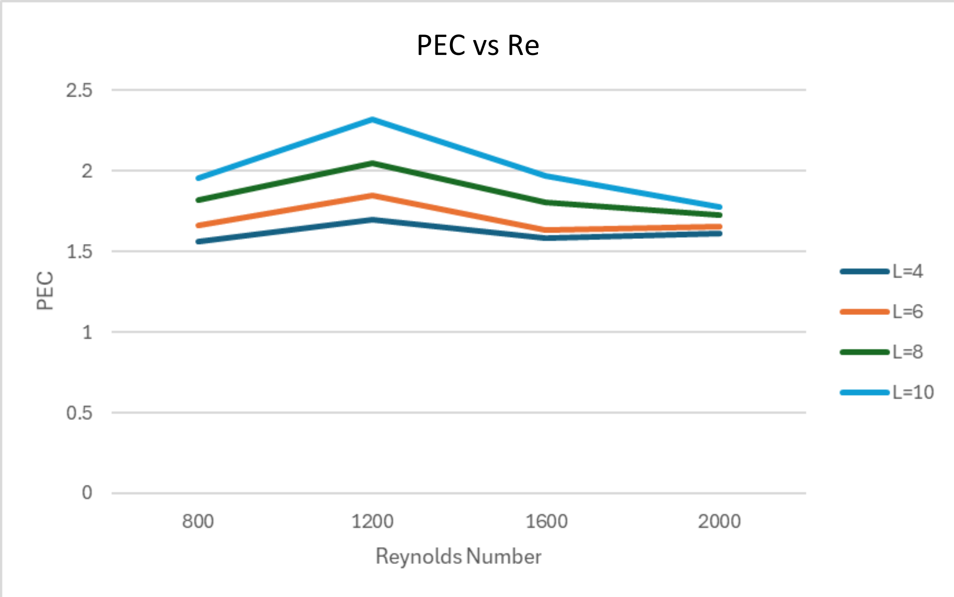

Figure 18: PEC for different lengths of triangular fins

As a result of PEC simulations, L=10 mm is selected since it is more efficient than other Length values as can be seen on Figure 18.

4.3 ANGLE EFFECT OF FINS ON HEAT TRANSFER AND NUSSELT NUMBER IN PIPE FLOW: THEROTICAL AND NUMERICAL INVESTIGATION DIFFERENT

In this part of the study, another geometry effect such as the angles (α) of the fin structures is examined with constant length. Then the most effective structure is selected and will be used in other analyses. In the analysis results obtained from different geometries, it has been observed that the best performance is achieved with the triangular fin. For an L length of 10 mm, the results for different angles (α) have been examined can be seen on Figure 19.

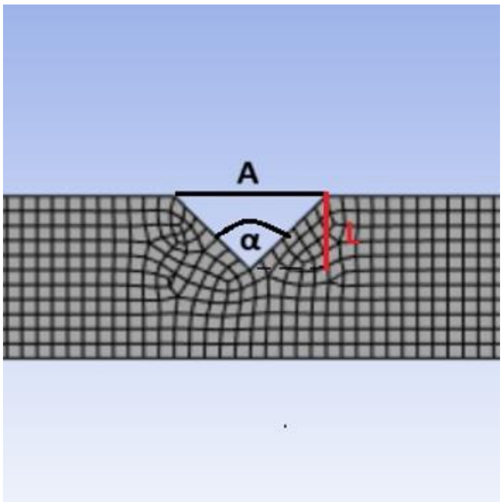

Figure 19: Representation of geometrical parameters of triangle fin

4 different angles (α) were examined in this thesis, and 16 different simulations were run. The fluid was determined to be water, and the analyses were carried out by considering the features in the length comparison. As can be seen in the table, the effects of different Reynolds numbers for 4 different angle values on the system were evaluated. The A (width) value was changed in the analysis. Angels were determined according to the width values that changed as 3, 5, 7, and 10 mm, respectively. In the length (L) experiment, the A (width) value was kept constant, and the analyses were made with a value of 3 mm.

Table 23: Results of Re, Nu and h for different angles of triangular fins

α = 17°			**α = 29°**			**α = 41°**			**α = 60°**		
Re	**Nu**	**h**	**Re**	**Nu**	**h**	**Re**	**Nu**	**h**	**Re**	**Nu**	**h**
800	16,3	409,2	800	15,2	428,8	800	14,7	355,1	800	13,9	435,0
1200	25,6	726,0	1200	22,5	522,7	1200	20,9	590,1	1200	19,9	595,6
1600	29,9	761,1	1600	27,2	714,7	1600	25,5	707,5	1600	24,5	710,7
2000	30,5	831,8	2000	29,7	805,0	2000	28,8	797,0	2000	27,2	799,2

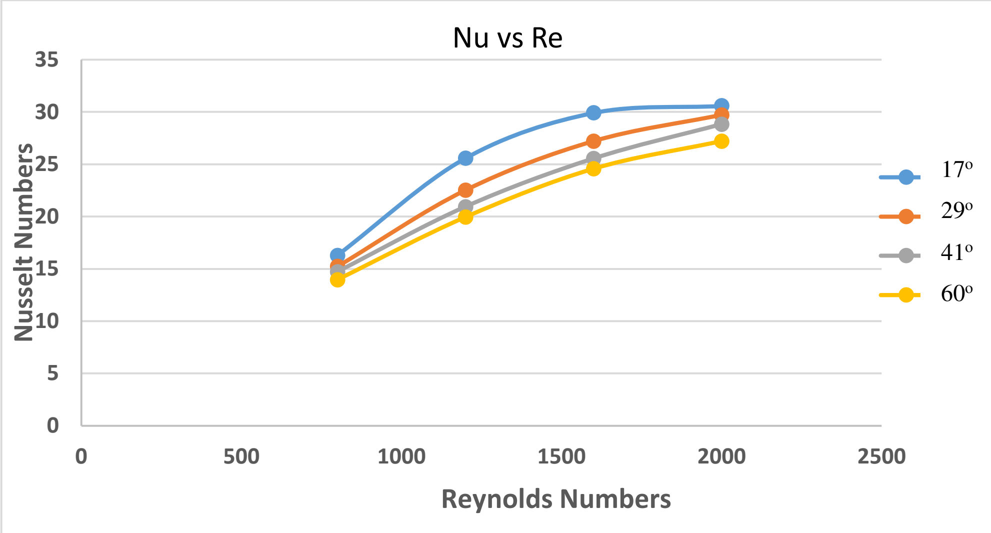

Figure 20: Triangle Fin's different angles results comparison graph

According to the results which can be seen on Table 23 and Figure 20, when the angle degree (α) increases, the heat transfer enhancement in the system is negatively affected, and there is an inverse proportion.

Heat transfer performance of triangular fin with different angles is studied using PEC analysis, and the results are shown in Figure 21.

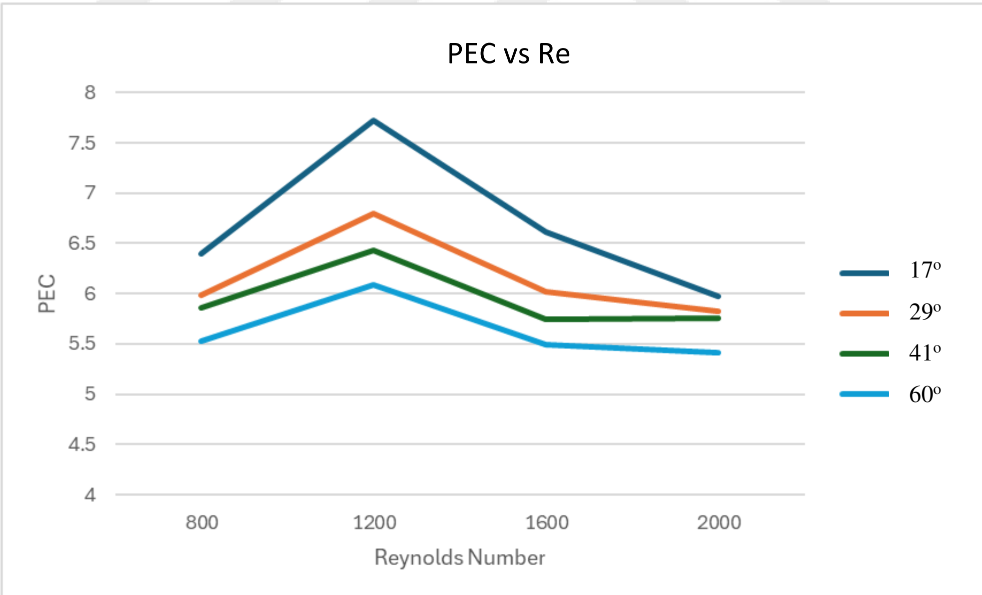

Figure 21: Triangle Fin's PEC comparison graph

According to Figure 21, it was observed that the first trial, in which the length value was equal to 10 mm and the angle (α) value was 17°, that is, the width was 3 mm, was more effective than the other fin structures. As a result, the triangular fin structure with a length of L = 10 mm and a width of w = 3 mm ($\alpha = 17°$) was selected as the most effective structure to be used in nanofluid analyses.

4.4 THE EFFECT OF NANOFLUID AND NANOPARTICLE CONCENTRATION ON HEAT TRANSFER ENHANCEMENT OF TRIANGULAR FINS

When various geometric analyses (such as length and angle) were completed among the fin structures using water as the heat transfer fluid. It was determined that the best structure was the triangular fin structure.

In this part, effect of nanofluids formed by mixing nanoparticles in various concentrations on triangular fins will be investigated.

These fluids are determined as Al_2O_3-TiO_2, Al_2O_3-Cu and TiO_2-MXene respectively and the concentration ratios of the nanoparticles are selected as: 2.5-1.5%,5-3%,10-6% and 3-5% respectively. Also, the base fluid was determined to be water.

The thermophysical properties of nanoparticles were found based on the formulas given before. The material properties used in these calculations, which were made by considering various concentration levels for each fluid, were also found during the literature review and were specified in the previous section. After these calculations, analyses were run using the ANSYS Fluent CFD program. Nanofluids at each concentration level are compared. The most effective nanofluids selected were compared with the most effective nanofluids is selected accordingly.

4.4.1 Water- Al_2O_3-TiO_2 Nanofluid's Heat Transfer Enhancement Effects on Triangle Fin Structured Tube Geometry

Firstly, aluminum oxide and titanium dioxide were added to the water-based fluid. After the particles were added, the fluid velocity was studied at Reynolds numbers of 800 to 2000, which is again the laminar region. The concentration ratios of the nanoparticles were analyzed as 2.5-1.5%,5-3%,10-6% and 3-5% respectively. As mentioned before, the geometric structure is a pipe with a length of 2200 mm and a diameter of 22 mm, and inside this pipe there are triangular fin structures with a length value equal to 10 mm and a width of 3 mm.

In the following sections, the effects of nanofluid flow on heat transfer coefficients and Nusselt numbers resulting from the change in nanoparticles are investigated.

Table 24 shows the effect of nanoparticle concentration ratios on the Nusselt number and heat transfer coefficient. Figure 22 also provides a comparison of these results, allowing the selection of the most effective nanofluid.

Table 24: Nusselt number and heat transfer coefficients of Al_2O_3-TiO_2 nanofluid

Al_2O_3 (2.5)-TiO_2(1.5) %			Al_2O_3 (5)- TiO_2 (3) %			Al_2O_3 (10)- TiO_2 (6) %			Al_2O_3 (3)- TiO_2 (5) %		
Re	**Nu**	**h**	**Re**	**Nu**	**h**	**Re**	**Nu**	**h**	**Re**	**Nu**	**h**
800	25,2	781,0	800	27,6	947,7	800	30,3	1272,7	800	25,1	855,5
1200	30,1	932,3	1200	32,0	1098,1	1200	34,5	1447,4	1200	30,0	1022,4
1600	34,0	1054,9	1600	36,4	1251,0	1600	39,8	1670,7	1600	33,9	1156,5
2000	39,4	1220,2	2000	42,3	1453,0	2000	46,5	1951,1	2000	39,3	1337,5

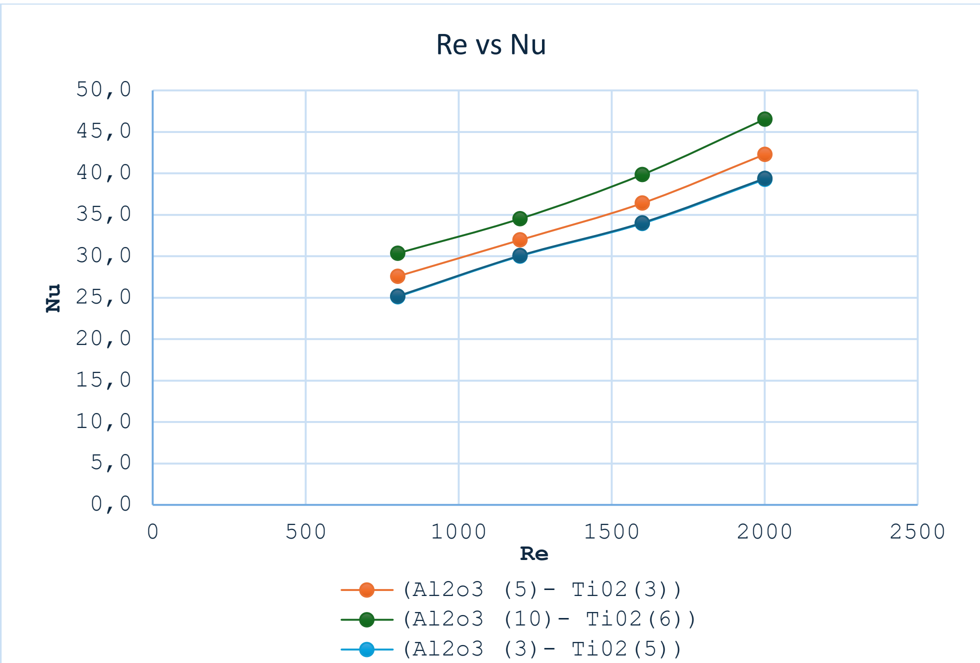

Figure 22: Comparison of concentration levels of Al_2O_3-TiO_2 nanofluid

When the results are examined, it is observed that when the particle concentration of the water -Al_2O_3- TiO_2 nanofluid increases, the Nusselt number and heat transfer coefficient also increase. In addition, Al_2O_3 or TiO_2 concentration levels were evaluated to be compared with each other, and it was observed that Al_2O_3 was more effective in the nanofluid where it was present in a higher percentage of concentration. As a result of simulations, Al_2O_3- TiO_2 was selected with 10-6% concentration because their Nusselt number and heat transfer coefficients are more effective as can be seen in Figure 22.

In the following section, the temperature and velocity contours can be seen for Re=800 and Re=2000 respectively in Figure 23 and 24.

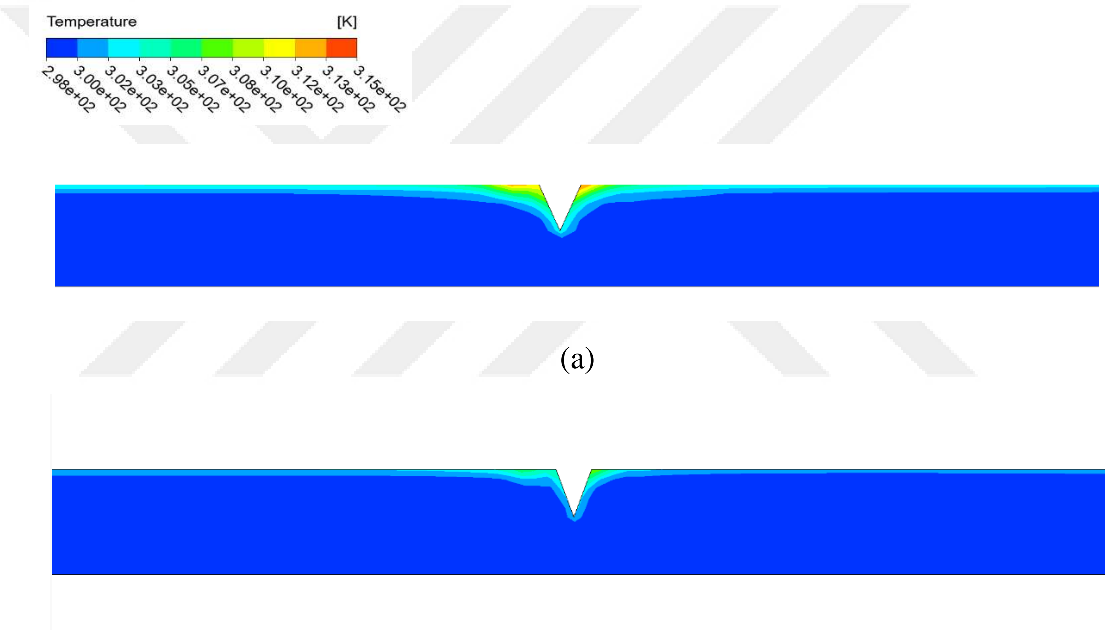

(a)

(b)

Figure 23: Temperature contours comparison of Al_2O_3-TiO_2 nanofluid with (a) Re=800 and (b) Re=2000

As can be seen in Figure 23, the temperature contours revealed a higher concentration of heat in the tube wall section, and heat transfer is lower at Re=800 compared to Re=2000. The enhanced heat transfer at Re=2000 resulted in stronger convection due to the constant heat applied to the wall. This led to a colder structure within and inside the pipe and near the fins, consequently reducing the temperature difference between the average fluid temperature and the wall temperature, thereby improving the heat transfer performance.

(a)

(b)

Figure 24: Velocity contours comparison of Al_2O_3-TiO_2 nanofluid with (a) Re=800 and (b) Re=2000

In Figure 24, velocity contour comparison with Re=800 and Re= 2000 is studied inside the pipe. Normally this study is carried out in the laminar region, but thanks to the fin structure added to the pipe, the fluid is accelerated and starts to behave as if it were in a turbulent regime. As can be seen in the velocity scale, the regime is outside the laminar region and the reason for this is that the flow area is narrowed by the fin geometry, and the fin structure acts as a turbulator, helping the fluid in the pipe to accelerate.

4.4.2 Water- Al_2O_3-Cu Nanofluid’s Heat Transfer Enhancement Effects on Triangle Fin Structured Tube Geometry

Firstly, aluminum oxide and copper were added to the water-based fluid. After the particles were added, the fluid velocity was studied at Reynolds numbers of 800 to 2000, which is again the laminar region. The concentration ratios of the nanoparticles are analyzed as 2.5-1.5%,5-3%,10-6% and 3-5% respectively. As mentioned before, the geometric structure is a pipe with a length of 2200 mm and a diameter of 22 mm, and inside this pipe there are triangular fin structures with a length value equal to 10 mm and a width of 3 mm. In the following sections, the effects of heat transfer coefficients and Nusselt numbers resulting from the change in nanoparticle concentration are investigated.

Table 25 shows the effect of nanoparticle concentration ratios on the Nusselt number and heat transfer coefficient. Figure 25 also provides a comparison of these results, allowing the selection of the most effective nanofluid.

Table 25: Nusselt number and heat transfer coefficients results of Al2O3-Cu nanofluid

Al_2O_3(2.5)- Cu(1.5)%			Al_2O_3 (5)- Cu(3) %			Al_2O_3 (10)- Cu(6) %			Al_2O_3 (3)- Cu(5) %		
Re	**Nu**	**h**	**Re**	**Nu**	**h**	**Re**	**Nu**	**h**	**Re**	**Nu**	**h**
800	24,4	761,6	800	26,2	915,4	800	28,5	1233,7	800	22,3	779,8
1200	29,5	920,5	1200	30,9	1076,8	1200	32,8	1417,1	1200	27,8	973,2
1600	33,3	1040,0	1600	35,0	1221,9	1600	37,5	1620,3	1600	31,5	1101,5
2000	38,4	1200,3	2000	40,6	1416,4	2000	43,6	1885,0	2000	36,1	1262,3

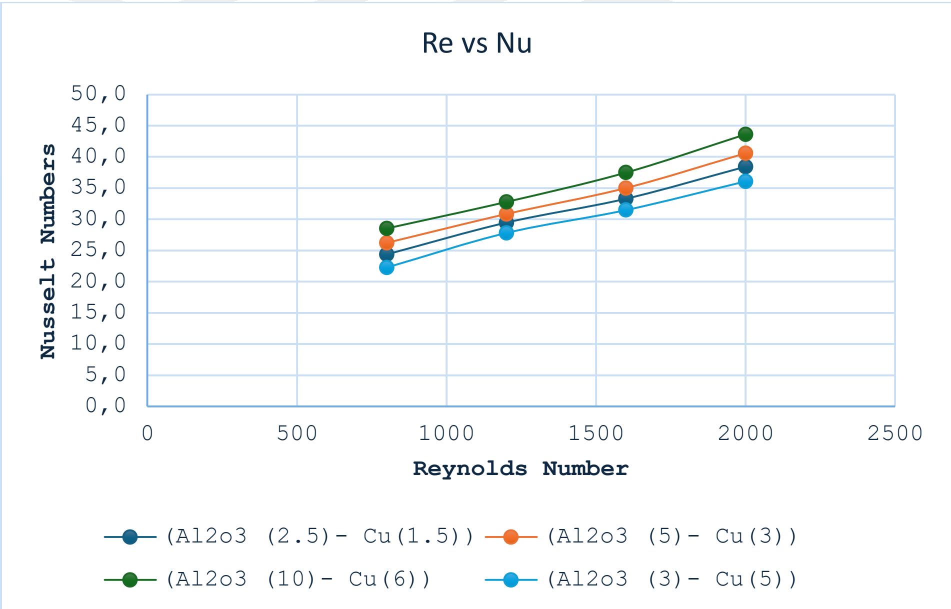

Figure 25: Comparison of concentration levels of Al_2O_3-Cu nanofluid

When the results are examined, it is observed that when the particle concentration of the water -Al_2O_3- Cu nanofluid increases, the Nusselt number and heat transfer coefficient also increase. In addition, Al_2O_3 or Cu concentration levels were evaluated to be compared with each other, and it was observed that Al_2O_3 was more effective in the nanofluid where it was present in a higher percentage of concentration. As a result of simulations, Al_2O_3- Cu was selected with 10-6%

concentration because their Nusselt number and heat transfer coefficients are more effective as can be seen in Figure 26.

In addition, temperature and velocity contours were taken by ANSYS, and the contour differences between Reynolds numbers 800 and 2000 were also examined. Details are explained in the following section.

In Figure 26, the temperature contours can be seen in the same section for Re=800 and Re=2000. Contours were obtained by keeping the temperature scale equal for a better understanding.

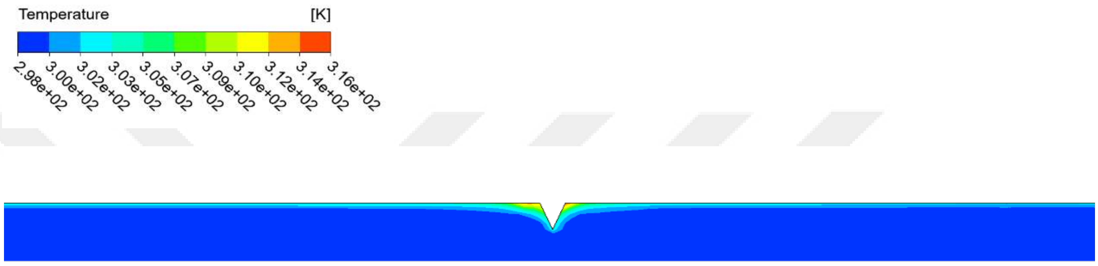

(a)

(b)

Figure 26: Temperature contours comparison of Al_2O_3-Cu nanofluid with (a) Re=800 and (b) Re=2000

As can be seen in Figure 26, the temperature contours revealed a higher concentration of heat in the tube wall section, and heat transfer is lower at Re=800 compared to Re=2000. The enhanced heat transfer at Re=2000 resulted in stronger convection due to the constant heat applied to the wall. This led to a colder structure inside the pipe and near the fins, consequently reducing the temperature difference between the average fluid temperature and the wall temperature, thereby improving the heat transfer performance. Comparison of the average fluid velocity values inside the pie for Re=800 and Re=2000 can be seen in Figure 27.

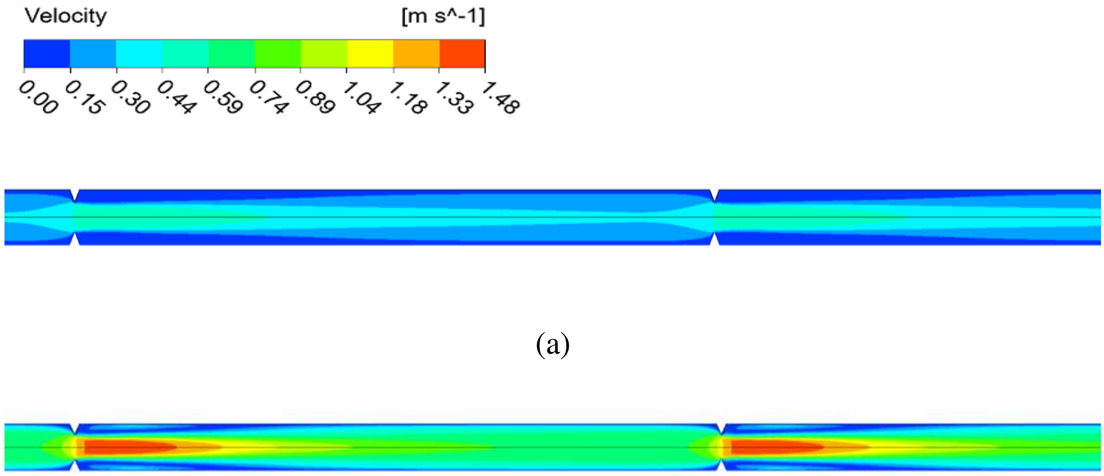

(a)

(b)

Figure 27: Velocity contours comparison of Al_2O_3-Cu nanofluid with (a) Re=800 and (b) Re=2000

It was observed that the velocity of the Al_2O_3-Cu mixture liquid is lower compared to the Al_2O_3-TiO_2 mixture. Because of fluid viscosity and thermophysical properties. The main factor can be stated as the low flow regime velocity due to the high viscosity of AL_2O_3-Cu liquid. Since the velocity decrease also influences heat transfer enhancement, the Nusselt number and heat transfer coefficient values for each concentration value of Al_2O_3-TiO_2 fluid are higher than Al_2O_3-Cu fluid.

4.4.3 Water- TiO_2-MXene Nanofluid's Heat Transfer Enhancement Effects on Triangular Fin Structured Tube Geometry

In this section, TiO_2-MXene mixed water based nanofluid is studied for Reynolds numbers of 800 to 2000 which is again the laminar region. The concentration ratios of the nanoparticles in them were analyzed as 2.5-1.5%,5-3%,10-6% and 3-5% respectively.

In other nano fluids, a significant increase in heat transfer properties was observed as the concentration of added nanoparticles increased, but in this fluid, a similar trend was not observed at different concentrations, i.e. as the concentrations increased. As seen in Table 26 and Figure 28, as the concentration level increased, the Nusselt number slightly decreased. While this was directly proportional to the other fluids, it was inversely proportional to this mixture.

Table 26: Nusselt number and heat transfer coefficients of TiO_2-MXene nanofluid

TiO_2 (2.5)-MXene (1.5) %			**TiO_2(5)-MXene(3) %**			**TiO_2 (10)-MXene(6) %**			**TiO_2 (3)-MXene(5) %**		
Re	**Nu**	**h**	**Re**	**Nu**	**h**	**Re**	**Nu**	**h**	**Re**	**Nu**	**h**
800	21,1	652,4	800	20,5	699,1	800	20,0	832,1	800	19,5	672,3
1200	26,8	629,2	1200	25,6	875,9	1200	25,9	1073,5	1200	25,3	874,5
1600	30,5	942,8	1600	29,9	1023,3	1600	29,6	1227,9	1600	29,1	1004,6
2000	34,8	1075,5	2000	34,1	1164,6	2000	33,6	1395,5	2000	33,0	1139,3

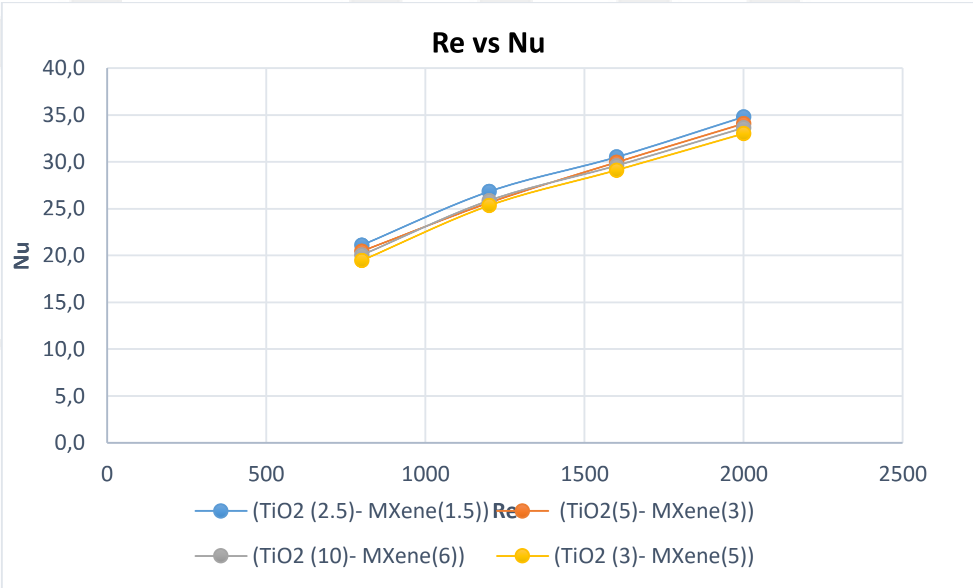

Figure 28: Comparison of concentration levels of TiO_2-MXene nanofluid

This negative effect of the increase in the level of nanoparticles added to the fluid on the Nusselt number, can be depicted regarding the viscosity of the MXene mixed nanofluid being high. Since the viscosity level influences the fluid speed, it also had a direct effect on the Nusselt number.

In other words, although the thermal conductivity level of the newly formed liquid showed similar trends as the previous ones, the viscosity high at high concentrations, which directly affected the heat transfer performance negatively.

4.5 COMPARISON OF DIFFERENT NANOFLUID WITH TRIANGULAR FINS

Al_2O_3-TiO_2 nanoparticles added to water at concentrations of 10–6% generally produced the best fluid that could be described within studied nanofluids and concentrations. Figure 29 shows the comparison of Nusselt numbers within different nanofluids. On the other hand, the passive technique employed, the Triangular Fins, result in pressure drops even the heat transfer increase by nature. Figure 30 shows the comparison of the friction factor values for different nanofluids.

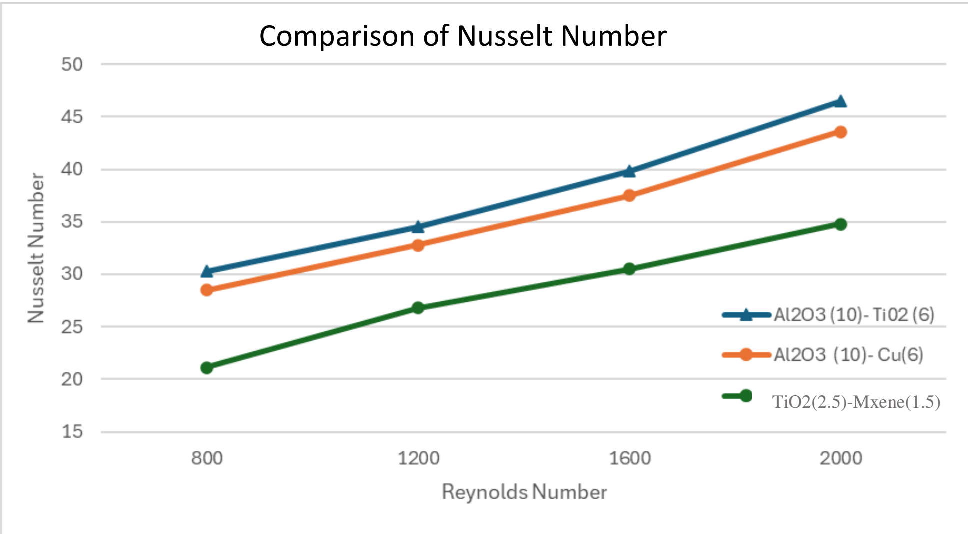

Figure 29: Comparison of Nusselt number for nanofluids

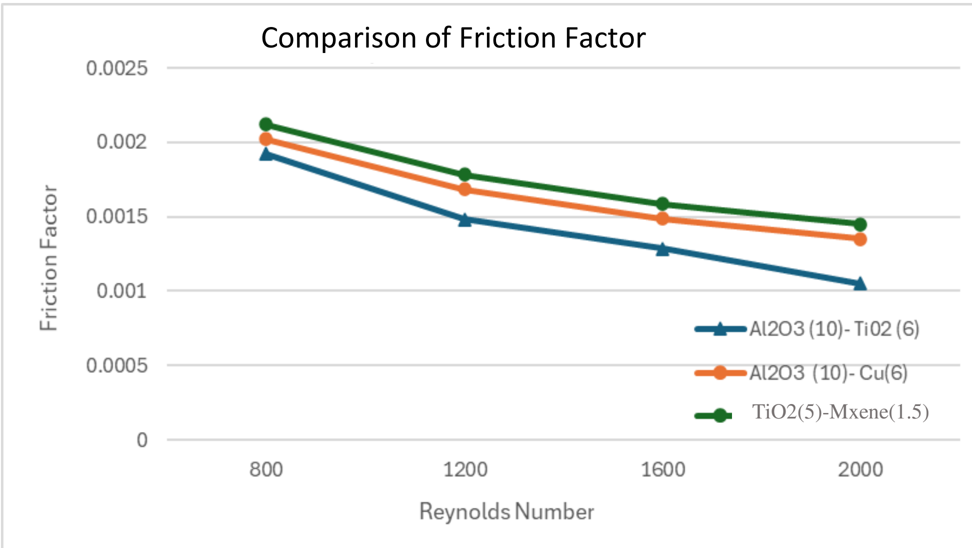

Figure 30: Comparison of friction factor for nanofluids

As a result, the most effective fin structure was determined as the triangular fin structure with various analyses and PEC results. The length was examined in the triangular fin structure and because of the PEC performed, it was observed that the triangular fin structure with the value of L=10 mm was effective. With this result, this triangular structure was used for the other geometrical examination, the width changes effect (angle change). As a result of the PEC calculations made in these analyses, the most efficient system was the triangular structure with an angle degree of 17, that is, as a result, it was seen that the most efficient system among the geometric factors and structures was the triangular structure with a length of L=10 mm and an angle of 17 degrees.

Then, nanofluid analysis was performed, 3 different types and 4 different concentrations of analyzes were performed and because of the analyses, the best system was the nanofluid with 10-6% concentration of Al_2O_3-TiO_2 nano particles.

As a result, the most effective system was the nanofluid with a triangular fin of L=10 mm length and 17-degree angle and 10-6% concentration of Al_2O_3-TiO_2 nano particles.

CHAPTER V
CONCLUSION

5.1 CONCLUSION OF STUDY

A numerical study was carried out to investigate the convective heat transfer characteristics, Nusselt number, friction factor and performance evaluation criteria (PEC) of differenties in fin geometry tubes (triangular, semicircular and rectangular) and with and without nanofluids such as Aluminum-Titanium Oxide (Al_2O_3-TiO_2), Aluminum -Copper (Al_2O_3-Cu) and Titanium Oxide- Mxene (TiO_2-Mxene).

Water-based nanofluids are used as heat transfer fluida and analyses are performed under constant heat flux, laminar flow regime, uniform inlet velocity and steady-state assumption. Numerical analyses were performed using ANSYS Fluent 24R2 software.

In the study, straight pipes and finned pipes with three different geometric structures with different dimensions are modeled and simulated by using.

Only water and different nanofluid concentration was intensively studied. (2.5%-1.5% for Al_2O_3-TiO_2, 5%-3% for Al_2O_3-Cu, 10%-6% and 3%-5% for TiO_2-MXene). Using these parameters, Nusselt number, friction factor and performance evaluation criterion (PEC) are investigated and the results are presented in tables and graphs. The Reynolds number range examined in the study is 800-2000 which corresponds to laminar flow regime.

First, analyses were performed with water in a straight pipe. Then, heat transfer of water in a fined geometry (semicircular, triangular, rectangular) pipe was investigated. After the optimum geometry is selected; which is the triangular fin geometry, different geometric parameters are studied.

As a result, when optimum triangular parameters are depicted, different nanofluids with different ratios are studied and optimum configuration is figured. According to the results, the Al_2O_3-TiO_2 based nanofluid with a concentration of 10%-6% compared to the other showed the highest Nusselt number and the lowest friction factor values of the analysis.

It was confirmed by the analysis that the friction factor and Nusselt number increased with the Reynolds number. In addition, it was observed that the finned tube showed a significant increase in heat transfer and also an increase in the friction factor compared to the smooth tube.

Observations in this area have shown that the "blockage phenomenon" occurs for higher "L" factors for triangles, rectangles and semicircles. Long fins can divide the flow path, causing flow separation and backflow instead of turbulence. This increases pressure loss, decreased heat transfer efficiency can decrease. This phenomenon causes more resistance to fluid flow and an increase in friction factor, which leads to a decrease in performance evaluation criteria (PEC).

The results of the study, considering the Performance Evaluation Criteria (PEC), the best performance case for all analyzed scenarios is summarized below:

- Geometric fin structure: In the geometries investigated in the analyses (triangle, circle, rectangle), the triangular structured geometry showed the best results. The results were examined by keeping the A and L values variable in the geometries.
- Triangular geometric fin structure: In the triangular fin, “L” value was kept constant and “A” was changed, and the α value was examined at the angles that changed with the change of “A”. Analyses were made with the best angle (α=17°).
- Effect of Nanofluid Concentration: Nanofluid with high concentration caused an observable increase in the Nusselt number compared to water, on the other hand, analysis showed that it increased the friction factor in the laminar flow case.
- Nanofluid Type: Among the nanofluids used and examined in the analyses (Al_2O_3-TiO_2, Al_2O_3-Cu and TiO_2-MXene), Al_2O_3-TiO_2 based nanofluid showed the best performance as a result of the studies. Al_2O_3-TiO_2 based nanofluid achieved the highest Nusselt number and provided a low friction factor. This nanofluid showed the most advantageous heat transfer properties with a concentration of 10-6%.
- Al_2O_3-TiO_2 Nanofluid: Increasing the Al_2O_3 concentration has shown results that improve heat transfer performance with this nanofluid.

- TiO_2-MXene Nanofluid: This nanofluid differed from other nanofluids used. The increase in particle concentration did not show a proportional increase in Nusselt number compared to others. The analysis has shown that the effect of viscosity value is significantly important in the heat transfer monitoring of this nanofluid. The smallest change in viscosity showed less change in Nusselt number and heat transfer compared to others.
- Blockage Phenomenon: At high “L” value, “blockage phenomenon” was observed. This situation may cause the finned tube flow path to block. This situation exhibited an increase in the friction factor and a decrease in the PEC value. The values greater than L=12 has a blockage condition and beyond that PEC state to decrease.

Among the different parameters examined in the study, it was observed that the thermophysical parameter that affects the heat transfer performance the most is viscosity. The analysis with PEC emphasized that it plays an important role in measuring and concluding the combined heat transfer and pressure drop performance. This study brings an innovative approach to the literature. The use of triangular geometric structured fins with Al_2O_3-TiO_2, Al_2O_3-Cu and TiO_2-MXene water-based nanofluids.

5.2 FUTURE STUDIES

Suggestions for Future Studies:

In future studies, the triangular finned tube examined in this study can actually be studied experimentally and the analyses can be performed experimentally.

A more comprehensive study can be done by physically measuring the heat transfer and flow behaviors with experimental investigations. During the experiment, pressure loss, inlet & outlet temperature, friction coefficient, heat transfer coefficient can be measured by experiment and Nusselt calculation can be made. Different results can be examined by changing the following parameters during the experiment.

- Different fin structures can be developed and included in the experiment
- Different concentrations and different nanofluids can be examined and used in the experiment.

An additional study that can be used in this experiment can be a heated test setup. The temperature change of the nanofluid or water passing through the finned tube under constant heat flux can be examined in detail. This test will play an important role in verifying the data obtained with numerical analysis.

REFERENCES

[1] PATHIPAKKA Govarthan and SIVASHANMUGAM Periyasamy (2010), "Heat Transfer Behaviour of Nanofluids in a Uniformly Heated Circular Tube Fitted with Helical Inserts in Laminar Flow", *International Journal of Heat and Mass Transfer*, Vol. 53, No. 21–22, pp. 4603–4611.

[2] BERGLES A. E. (1988), "Some Perspectives on Enhanced Heat Transfer, Second-Generation Heat Transfer Technology", *ASME Journal of Heat Transfer*, Vol. 110, pp. 1082–1096.

[3] HERIS S. Zeinali, ETEMAD S. Gh and ESFAHANY M. Nasr (2006), "Experimental Investigation of Oxide Nanofluids Laminar Flow Convective Heat Transfer", *International Communications in Heat and Mass Transfer*, Vol. 33, No. 4, pp. 529–535.

[4] ROHSENOW Warren M., HARTNETT James P. and CHO Young I. (1998) *Handbook of heat transfer*, Mcgraw-Hill, New York.

[5] WEN Dongsheng and DING Yulong (2004), "Experimental Investigation into Convective Heat Transfer of Nanofluids at the Entrance Region Under Laminar Flow Conditions", *International Journal of Heat and Mass Transfer*, Vol. 47, pp. 5181–5188.

[6] CHOI S. Us and EASTMAN Jeffrey A. (1995), *Enhancing thermal conductivity of fluids with nanoparticles*, Argonne National Laboratory, No. ANL/MSD/CP-84938; CONF-951135-29, IL, United States.

[7] HERIS S. Zeinali, ETEMAD S. Gh, and ESFAHANY M. Nasr (2006), "Experimental Investigation of Oxide Nanofluids Laminar Flow Convective Heat Transfer", *International Communications in Heat and Mass Transfer*, Vol. 33, No. 4, pp. 529–535.

[8] MAIGA Sidi El Becaye, PALM Samy Joseph, NGUYEN Cong Tam, ROY Gilles and GALANIS Nicolas (2005), "Heat Transfer Enhancement by Using Nanofluids in Forced Convection Flows", *International Journal of Heat and Fluid Flow*, Vol. 26, pp. 530–546.

[9] LI Q. and XUAN Yimin (2000), *Heat Transfer Science and Technology*, Higher Education Press, Newyork.

[10] WANG Xiang-Qi and MUJUMDAR Arun S. (2007), “Heat Transfer Characteristics of Nanofluids: A Review”, *International Journal of Thermal Sciences*, Vol. 46, pp. 1–19.

[11] EASTMAN Jeffrey, A. PHILLPOT S. R., CHOI S. U. S. and KEBLINSKI P. (2004), “Thermal Transport in Nanofluids”, *Annual Review of Materials Research*, Vol. 34, pp. 219–246.

[12] DAS Sarit K., CHOI Stephen U. S., YU Wenhua and PRADEEP T. (2008), *Nanofluids: Science and Technology*, Wiley-Interscience, Hoboken, NJ.

[13] SIVASHANMUGAM Periyasamy (2012), *An Overview of Heat Transfer Phenomena*, Higher Education Press, Newyork.

[14] GRANQVIST Claes-Göran, BUHRMAN Raymond A., WYNS J. and SIEVERS Albert J. (1976), “Far-Infrared Absorption in Ultrafine Al Particles”, *Physical Review Letters*, Vol. 37, No. 10, pp. 625.

[15] PORDANJANI Ali Hossein, AGHAKHANI Saeed, AFRAND Mohammad, MAHMOUDI Behzad, MAHIAN Omid and WONGWISES Somchai (2019), “An Updated Review on Application of Nanofluids in Heat Exchangers for Saving Energy”, *Energy Conversion and Management,* Vol. 198, pp. 111886.

[16] SHEREMET Mikhail Alexandrovich. (2021), “Applications of Nanofluids”, *Nanomaterials*, Vol. 11, No. 7, pp. 1716.

[17] ASSAEL Marc J., ANTONIADIS Konstantinos D., WAKEHAM William A. and ZHANG Xianfan (2019), “Potential Applications of Nanofluids for Heat Transfer”, *International Journal of Heat and Mass Transfer*, Vol. 138, pp. 597–607.

[18] YU Wenhua, FRANCE David M., ROUTBORT Jesse L. and CHOI Stephen U. S. (2008), “Review and Comparison of Nanofluid Thermal Conductivity and Heat Transfer Enhancements”, *Heat Transfer Engineering*, Vol. 29, No. 5, pp. 432–460.

[19] FARHANA Khadijah, KADIRGAMA Kulanthayan, RAHMAN Md. Mustafizur, NOOR Mohd. Mamat, RAMASAMY Durairaj, SAMYKANO Mutharasan (2019), “Significance of Alumina in Nanofluid Technology: An Overview”, *Journal of Thermal Analysis and Calorimetry*, Vol. 138, pp. 1107–1126.

[20] ANITHA Subramanian, THOMAS Tharves, PARTHIBAN Vijay and PICHUMANI Manikandan (2019), "What Dominates Heat Transfer Performance of Hybrid Nanofluid in Single Pass Shell and Tube Heat Exchanger?", *Advanced Powder Technology*, Vol. 30, No. 12, pp. 3107–3117.

[21] YOUNES Hassan, MAO Meng, MURSHED Sajjad S., LOU Dong, HONG Haihong and PETERSON Goran P. (2022), "Nanofluids: Key Parameters to Enhance Thermal Conductivity and Its Applications", *Applied Thermal Engineering*, Vol. 207, pp. 118202.

[22] AKOH Hiroshi, TSUKASAKI Yoshio, YATSUYA Seiji and TASAKI Akira (1978), "Magnetic Properties of Ferromagnetic Ultrafine Particles Prepared by Vacuum Evaporation on Running Oil Substrate", *Journal of Crystal Growth*, Vol. 45, pp. 495–500.

[23] GÜRMEN Süleyman ve EBİN Bülent (2008), "Nanopartiküller ve Üretim Yöntemleri-1", *Metalurji Dergisi*, Vol. 150, pp. 31–38.

[24] HUA Yong-Chang and CAO Bin-Yu. (2017), "An Efficient Two-Step Monte Carlo Method for Heat Conduction in Nanostructures", *Journal of Computational Physics*, Vol. 342, pp. 253–266.

[25] ŞAHİN Fikret ve NAMLI Levent (2018), "Nanoakışkanlarda Kararlılığın Isı Transferini İyileştirme Açısından Önemi", *Niğde Ömer Halisdemir Üniversitesi Mühendislik Bilimleri Dergisi,* Cilt 7, Sayı 2, ss. 880–898.

[26] YU Wenhua and XIE Hao (2012), "A Review on Nanofluids: Preparation, Stability Mechanisms, and Applications", *Journal of Nanomaterials*, Vol. 2012, pp. 435873.

[27] MOHAMMED Hussain. A., AL-ASWADI Abdullah A., SHUAIB Nasser. H. and SAIDUR Rashid (2011), "Convective Heat Transfer and Fluid Flow Study Over a Step Using Nanofluids: A Review", *Renewable and Sustainable Energy Reviews*, Vol. 15, No. 6, pp. 2921–2939.

[28] HUSSIEN Ammar A., ABDULLAH Mohd Zulkifli and MOH'D A. A. N. (2016), "Single-Phase Heat Transfer Enhancement in Micro/Minichannels Using Nanofluids: Theory and Applications", *Applied Energy*, Vol. 164, pp. 733–755.

[29] CHAKRABORTY Sourav and PANIGRAHI Prabir Kumar (2020), "Stability of Nanofluid: A Review", *Applied Thermal Engineering*, Vol. 174, pp. 115259.

[30] PORDANJANI Amir Hossein, AGHAKHANI Saeid, AFRAND Mohammad, SHARIFPUR Morteza, MEYER J. P., XU Hao (2021), "Nanofluids: Physical Phenomena, Applications in Thermal Systems and the Environment Effects – A Critical Review", *Journal of Cleaner Production*, Vol. 320, pp. 128573.

[31] CHANG Hsin, LO Chih-Hung, TSUNG Ting-Ting, CHO Yu-Ying, TIEN Dah-Chuan, CHEN Li-Chun ve THAI Chih-Hsiung (2005), "Temperature Effect on the Stability of CuO Nanofluids Based on Measured Particle Distribution", *Key Engineering Materials*, Vol. 295, pp. 51–56.

[32] SANI Emanuele, MERCATELLI Luca, BARISON Simone, PAGURA Cristina, AGRESTI Francesco, COLLA Luigi and SANSONI Paolo (2011), "Potential of Carbon Nanohorn-Based Suspensions for Solar Thermal Collectors", *Solar Energy Materials and Solar Cells*, Vol. 95, No. 11, pp. 2994–3000.

[33] AL-WAELI Ali H., CHAICHAN M. T., KAZEM Hussain. A. and SOPIAN Khalid (2019), "Evaluation and Analysis of Nanofluid and Surfactant Impact on Photovoltaic-Thermal Systems", *Case Studies in Thermal Engineering*, Vol. 13, pp. 100392.

[34] ELIAS Muammer M., MIQDAD Mohamed, MAHBUBUL Iftekhar M., SAIDUR Rafidah, KAMALISARVESTANI Mehdi, SOHEL Mohammed R. (2013), "Effect of Nanoparticle Shape on the Heat Transfer and Thermodynamic Performance of a Shell and Tube Heat Exchanger", *International Communications in Heat and Mass Transfer*, Vol. 44, pp. 93–99.

[35] PAK Bong Cheol and CHO Young Ik (1998), "Hydrodynamic and Heat Transfer Study of Dispersed Fluids with Submicron Metallic Oxide Particles", *Experimental Heat Transfer: An International Journal*, Vol. 11, No. 2, pp. 151–170.

[36] ARICI Müslüm, KAPTAN Çağatay ve KARABAY Hasan (2016), "Mixed Convection Heat Transfer of Nanofluids in a Trapezoidal Cavity Having an Adiabatic Square Body at Its Center", *Res. Eng. Struct. Mat.*, Vol. 3, No. 2, pp. 155- 162.

[37] AKÇAOĞLU Engin, ARICI Müslüm ve ÖĞÜT Elif Büyük (2012), "Bölmeli Bir Kare Kapalı Ortam İçindeki Nanoakışkanın Doğal Konveksiyonla Isı Transferinin Sayısal Olarak İncelenmesi", *Erciyes Üniversitesi Fen Bilimleri Enstitüsü Fen Bilimleri Dergisi*, Vol. 28, No. 5, pp. 359–366.

[38] ÖĞÜT Elif Büyük (2010), "Eğik Kare Kapalı Bir Bölge İçindeki Su Bazlı Nanoakışkanların Doğal Taşınımla Isı Transferi", *Isı Bilimi ve Tekniği Dergisi*, Vol. 30, No. 1, pp. 23–33.

[39] XUAN Yulong and LI Qinghua (2003), "Investigation on Convective Heat Transfer and Flow Features of Nanofluids", *Journal of Heat Transfer*, Vol. 125, No. 1, pp. 151–155.

[40] ÖĞÜT Elif Büyük (2009), "Natural Convection of Water-Based Nanofluids in an Inclined Enclosure with a Heat Source", *International Journal of Thermal Sciences*, Vol. 48, No. 11, pp. 2063–2073.

[41] ABU-NADA Eyad, ZIYAD Khaled, SALEH Mohammad and ALI Yasser (2008), "Heat Transfer Enhancement in Combined Convection Around a Horizontal Cylinder Using Nanofluids", *Heat Transfer*, Vol. 130, No. 8, pp. 84505.

[42] SUSANTEZ Çiğdem ve KAHVECİ Kamil (2017), "Numerical Investigation of Buoyancy Driven Heat Transfer of Water-Based CuO Nanofluids in a Rectangular Enclosure with an Offcenter Solid Conducting Body", *Isı Bilimi ve Tekniği Dergisi*, Vol. 37, No. 2, pp. 109–127.

[43] GHASEMI B. and AMINOSSADATI S. M. (2010), "Mixed Convection in a Lid-Driven Triangular Enclosure Filled with Nanofluids", *International Communications in Heat and Mass Transfer*, Vol. 37, No. 8, pp. 1142–1148.

[44] ÖZEL Cihan, MACİT Cevher Kürşat, TAŞKIRAN Ali ve ÖZEL Meral (2022), "Kendinden Helisel Kanatlı Boruların Isı Transfer Performansını Artırmaya Yönelik Yeni Bir Yaklaşım", *Fırat Üniversitesi Fen Bilimleri Dergisi*, Vol. 34, No. 2, pp. 113–127.

[45] EL MAAKOUL Anas, FEDDI Kawtar, SAADEDDINE Said, ABDELLAH Abdellatif Ben and EL METOUI Mustapha (2020), "Performance Enhancement of Finned Annulus Using Surface Interruptions in Double-Pipe Heat Exchangers", *Energy Conversion and Management*, Vol. 210, pp. 112710.

[46] HOSSEINI Mohammad Javad, RANJBAR Ali Akbar, RAHIMI Mohammad and BAHRAMPOURY Kambiz (2015), "Experimental and Numerical Evaluation of Longitudinally Finned Latent Heat Thermal Storage Systems", *Energy and Buildings*, Vol. 99, pp. 263–272.

[47] KIM Chang-Nam, JEONG Jin and YOUN Byung (2003), “Evaluation of Thermal Contact Conductance Using a New Experimental-Numerical Method in Fin-Tube Heat Exchangers”, *International Journal of Refrigeration*, Vol. 26, No. 8, pp. 900–908.

[48] KOTCIOĞLU İsak ve BÖLÜKBAŞI Abdurrahim (2003), “Düşey Dikdörtgen Kesitli Bir Kanalda Farklı Kanatçıklı Yüzeylerde Isı Transferinin İncelenmesi”, *Dokuz Eylül Üniversitesi Mühendislik Fakültesi Fen ve Mühendislik Dergisi*, Vol. 5, No. 2, pp. 89–102.

[49] EREK Aytunç, ÖZERDEM Barış, BİLİR Levent and İLKEN Zafer (2005), “Effect of Geometrical Parameters on Heat Transfer and Pressure Drop Characteristics of Plate Fin and Tube Heat Exchangers”, *Applied Thermal Engineering*, Vol. 25, No. 14–15, pp. 2421–2431.

[50] ŞAHİN Hacı Mehmet, DAL Ali Rıza and BAYSAL Eşref (2007), “3-D Numerical Study on the Correlation Between Variable Inclined Fin Angles and Thermal Behavior in Plate Fin-Tube Heat Exchanger”, *Applied Thermal Engineering*, Vol. 27, No. 11–12, pp. 1806–1816.

[51] BAZARBASHI Milad (2013), *Dalgalı Kanatçıklı Isı Değiştiricinin Yanıt Yüzey Metodu ile Çok Amaçlı Optimizasyonu* (Master’s Thesis), Atatürk Üniversitesi Fen Bilimleri Enstitüsü, Erzurum.

[52] BUYRUK Ertan and KARABULUT Koray (2013), “Numerical Investigation into Heat Transfer for Three-Dimensional Plate Fin Heat Exchangers with Fins Placed Perpendicular to Flow”, *Transactions of FAMENA*, Vol. 37, No. 2, pp. 87–102.

[53] BUYRUK Ertan ve KARABULUT Koray (2017), “Plakalı Kanatçıklı Isı Değiştiricilerde Kanat Geometrisinin Isı Transferine Olan Etkisinin Üç Boyutlu Sayısal Olarak İncelenmesi”, *Dokuz Eylül Üniversitesi Mühendislik Fakültesi Fen ve Mühendislik Dergisi*, Vol. 19, No. 56, pp. 346–363.

[54] KARATAŞ Tuğçe (2019), *CFD Analysis of Shell and Tube Heat Exchanger* (Yüksek Lisans Tezi), İnönü Üniversitesi Fen Bilimleri Enstitüsü, Malatya.

[55] CÜCE Erdem (2020), “Boyuna Uzatılmış Yüzeylerde Dikdörtgensel Oyukların Isı Atımına Etkisi: Bir Hesaplamalı Akışkanlar Dinamiği Analizi”, *Afyon Kocatepe Üniversitesi Fen ve Mühendislik Bilimleri Dergisi*, Vol. 20, No. 5, pp. 931–940.

[56] KOCA Tarkan ve BUDAK Serbay Ali (2021), “Kanatçıklı İç Borulu Dikey Isı Değiştiricilerde Isı Transferi ve Basınç Düşümü Analizi”, *Gümüşhane Üniversitesi Fen Bilimleri Dergisi*, Vol. 11, No. 1, pp. 62–72.

[57] IŞIK Erdem ve TUĞAN Volkan (2021), “Dairesel Bir Boruda Kullanılan Boyuna Dalgalı Kanatçıkların Isı Transferine Etkisinin Sayısal Olarak İncelenmesi”, *International Journal of Pure and Applied Sciences*, Vol. 7, No. 1, pp. 19–26.

[58] BUYRUK Ertan ve KARABULUT Koray (2020), “Research of Heat Transfer Augmentation in Plate Fin Heat Exchangers Having Different Fin Types”, *Journal of Engineering Thermophysics*, Vol. 29, pp. 316–330.

[59] TEPE Ahmet Ümit (2021), “Kanatlı-Borulu Isı Değiştiricilerinde Çukurlu/Çıkıntılı Kanat ile Isı Transfer Performansının Arttırılması”, *Avrupa Bilim ve Teknoloji Dergisi*, Vol. 23, pp. 401–414.

[60] PARLAK Nezaket ve ÇELİK Halime (2018), “Kanatçık Geometrisinin Isı Geçişine Etkisinin Parametrik İncelenmesi”, *International Journal of Multidisciplinary Studies and Innovative Technologies*, Vol. 2, No. 2, pp. 25–29.

[61] ABDULATEEF Ammar M., MAT Sahif., SOPIAN Kamaruzzaman, ABDULATEEF Jasim and GITAN Ali A. (2017), “Experimental and Computational Study of Melting Phase-Change Material in a Triplex Tube Heat Exchanger with Longitudinal/Triangular Fins”, *Solar Energy*, Vol. 155, pp. 142–153.

[62] KAZEMI M, HOSSEINI M. J., RANJBAR A. A. and BAHRAMPOURY Kambiz (2018), “Improvement of Longitudinal Fins Configuration in Latent Heat Storage Systems”, *Renewable Energy*, Vol. 116, pp. 447–457.

[63] ÇENGEL Yunus A. (2014), *Heat and Mass Transfer: Fundamentals and Applications*, McGraw-Hill, Newyork.

[64] LORENZINI Enrico, SPIGA Marco and FABBRI G. P. (1994), “A Polynomial Fin Profile Optimization”, *International Journal of Heat and Technology*, Vol. 12, pp. 137–144.

[65] FABBRI Giampietro (1998), “Heat Transfer Optimization in Internally Finned Tubes Under Laminar Flow Conditions”, *International Journal of Heat and Mass Transfer*, Vol. 41, No. 10, pp. 1243–1253.

[66] BABAR Hafeez, SAJID Muhammad Usman and ALI Hafiz M. (2019), "Viscosity of Hybrid Nanofluids: A Critical Review", *Thermal Science*, Vol. 23, No. 3B, pp. 1713–1754.

[67] ALI Hafız M., BABAR Hafeez, SHAH Tahir R., SAJID Muhammad Usman, QASIM Muhammad A. and JAVED Saeed (2018), "Preparation Techniques of TiO_2 Nanofluids and Challenges: A Review", *Applied Sciences*, Vol. 8, No. 4, pp. 587.

[68] GÖKTEPE Sinan, ATALIK Kunt and ERTÜRK Hakan (2014). "Comparison of single and two-phase models for nanofluid convection at the entrance of a uniformly heated tube.", *International Journal of Thermal Sciences*, Vol. 80, pp. 83-92.

[69] HO C.J., CHANG Chiayuan, YAN Wei Mon and AMANI Pouria (2018), "A combined numerical and experimental study on the forced convection of Al2O3-water nanofluid in a circular tube", *International Journal of Heat and Mass Transfer*, Vol. 120, pp. 66-75.

[70] XUAN Yimin and ROETZEL Wilfried (2000), "Conceptions for heat transfer correlation of nanofluids", *International Journal of Heat and Mass Transfer*, Vol. 43, Issue 19, pp. 3701-3707.

[71] TAWFIK Mohamed M. (2017), "Experimental Studies of Nanofluid Thermal Conductivity Enhancement and Applications: A Review", *Renewable and Sustainable Energy Reviews*, Vol. 75, pp. 1239–1253.

[72] BRAILSFORD A.D. MAJOR K.G. (1964), "The thermal conductivity of aggregates of several phases", including porous materials", *British Journal of Applied Physics*, Vol.15, No. 3, pp. 313-319.

[73] ÇENGEL Yunus A. and GHAJAR Afshin J. (2014), *Heat and mass transfer: fundamentals and applications*, 5th Edition, McGraw-Hill Higher Education, New York.

[74] GEE, Dennis Leroy and WEBB, R. L. (1980). "Forced convection heat transfer in helically rib-roughened tubes", *International Journal of Heat and Mass Transfer*, Vol. 23, No 8, pp. 1127-1136.

[75] KAKAÇ Sadık, YENER Yaman and PRAMUANJAROENKIJ Achasa (2014), Convective heat transfer, 3rd Edition, CRC Press Taylor & Francis Group, New York.

[76] SAVEKAR Avinash, JANGID Dhiraj, GURJAR Madhura, PATIL Vikrant and SEWATKAR C. M. (2015), "Analysis of Heat Transfer in Pipe with Twisted Tape Inserts", *Proceedings of the 2nd International Conference on Fluid Flow, Heat and Mass Transfer*, Paper No. 143, pp. 1-8, Ottawa, Ontario, Canada.

[77] ALSHEHRI Fahad, GORANIYA Jaydeep and COMBRINCK Madeleine L. (2020) "Numerical investigation of heat transfer enhancement of a water/ethylene glycol mixture with A12O3–TiO2 nanoparticles", *Applied Mathematics and Computation*, Vol. 369, Article 1248.

[78] YILMAZ Ömür ÇAKMAK (2025), *Synergistic Effects of Twisted Tape Geometry and Nanoparticles on Heat Transfer Performance in Tubes* (Master's Thesis), Çankaya Üniversitesi, Ankara.